이학박사학위논문

Macroscopic Quantum Superpositions in Many-Particle Systems

많은입자 계에서의 거시양자중첩

2017년 2월

서울대학교 대학원
물리·천문학부
박 채 연

Macroscopic Quantum Superpositions in Many-Particle Systems

Chae-Yeun Park

Supervised by

Associate Professor **Hyunseok Jeong**

A Dissertation

Submitted to the Faculty of

Seoul National University

in Partial Fulfillment of

the Requirements for the Degree of

Doctor of Philosophy

Feb. 2017

Department of Physics and Astronomy

The Graduate School

Seoul National University

Abstract

Macroscopic Quantum Superpositions in Many-Particle Systems

Chae-Yeun Park
Department of Physics and Astronomy
The Graduate School
Seoul National University

Quantum superpositions between macroscopically distinct objects, as illustrated in Scödinger's famous cat paradox, is not prohibited by the law of quantum mechanics but hardly seen in real everyday life. Decoherence theory is one of the most well-known argument to explain this paradox based on the interaction between the system of our interest and a big another system, which is usually called as bath or environment. The open system picture is sufficient for usual systems but conceptually incomplete as it is based on the *a priori* assumption that an environment is in an incoherent thermal state.

In this thesis, we investigate why it is so hard to see macroscopic superpositions without assuming a system is open. We offer two different viewpoints, based on the kinematics and the dynamics of a many-particle system, respectively. We consider pure states in many-particle spin-$1/2$ systems to simplify the investigation. We first introduce a measure of quantum macroscopicity for

this system which can be used as a criterion of a macroscopic superposition and compare it with the geometric measure of entanglement. From analytic observations using random matrix theory and extensive numerical calculations, we next show that random states in the many-particle Hilbert space typically have small quantum macroscopicity which means the rareness of macroscopic superpositions. This result gives a kinematical point of view answer why we cannot see Scödinger's cat in macroscopic systems.

We also obtain a similar result from the dynamics of a system. We introduce the concept of thermalization in a closed system and apply eigenstate thermalization hypothesis to show that the measure of quantum macroscopicity is small after thermalization. Extensive numerical results of quantum macroscopicity are also presented using the disordered XXZ model which alters between thermalization phase and many-body localized (MBL) phase. Consistent results are obtained that initial macroscopic superpositions that undergo thermalization disappear while they could be preserved in the MBL phase in which thermalization does not occur.

Keywords : Macroscopic quantum superpositions, Macroscopic quantum coherence, Typicality of quantum states, Thermalization, Many-body localization
Student Number : 2010-23146

Contents

List of Figures

List of Symbols

State kets of qubit (spin-$1/2$):

$$|0\rangle = |\uparrow\rangle = \begin{pmatrix} 1 \\ \\ 0 \end{pmatrix}, \qquad |1\rangle = |\downarrow\rangle = \begin{pmatrix} 0 \\ \\ 1 \end{pmatrix}$$

Pauli operators (gates):

$$\sigma_x = X = \begin{pmatrix} 0 & 1 \\ \\ 1 & 0 \end{pmatrix}, \quad \sigma_y = Y = \begin{pmatrix} 0 & -i \\ \\ i & 0 \end{pmatrix}, \quad \sigma_z = Z = \begin{pmatrix} 1 & 0 \\ \\ 0 & -1 \end{pmatrix}$$

The W and the GHZ states of three qubits:

$$|W\rangle = \frac{1}{\sqrt{3}}\big(|001\rangle + |010\rangle + |100\rangle\big)$$
$$|\mathrm{GHZ}\rangle = \frac{1}{\sqrt{2}}\big(|000\rangle + |111\rangle\big)$$

The W and the GHZ states of N qubits:

$$|W\rangle_N = \frac{1}{\sqrt{N}}\big(|0\cdots01\rangle + |0\cdots10\rangle + \cdots + |10\cdots0\rangle\big)$$
$$|\mathrm{GHZ}\rangle_N = \frac{1}{\sqrt{2}}\big(|0\rangle^{\otimes N} + |1\rangle^{\otimes N}\big)$$

Chapter 1

Introduction

Quantum mechanics contains many paradoxes that cannot be understood under the notion of classical physics. Among them, the Einstein-Podolsky-Rosen (EPR) [1] and the Schrödinger's cat [2] paradoxes are the most famous ones. The EPR paradox was proposed to argue that quantum mechanics is incomplete in the sense that it conflicts with local realism which we experience in everyday life. The paradox had not been well understood until John Bell's paper published in 1964 [3]. In his paper, Bell presented the basic assumptions of a local realistic theory and devised an inequality which is fulfilled under the assumptions but can be violated in quantum mechanics. There have been many different experiments that test the inequality and many physicists now agree that quantum mechanics exhibits some non-local behaviors.

Many years after the Bell's inequality, the evolution of quantum information theory more firmly established the way to quantify the amount of non-local correlations which a quantum state have. This quantification is based on the number of maximally entangled states that can be obtained from the many copies of the given state using local operations and classical communications (LOCC). This framework, including more general axiomatic extension, is usually referred as "entanglement monotone" or "LOCC monotone" and have succeeded incredibly and opened a new way to investigate various quantum non-

local phenomena. There are still some ambiguous points when we extend this framework to multipartite cases, but most physicists would agree that the entanglement for bipartite two-level (or qubit) system which is originally considered by Bell is well understood nowadays.

In contrast, the Schrödinger's cat paradox is still enigmatic compared to the EPR one despite the equally long history. In fact, there was an effort to devise the inequality similar to Bell's one from the assumption of macroscopic realism by Leggett and Garg [4]. This inequality is named after the authors, so called Leggett-Garg inequality. However, even though there have been many following works using this inequality, the meaning of "macroscopic" realism which is the basic assumption for Leggett-Garg inequality not much clear. For example, there would be some questions, like: "How much large is macroscopic?" or "Measuring individual particle can reveal macroscopic realism?" [5].

Experimentalists took a different way to attack the question. They have invested a lot of effort to make a bigger size of Schrödinger's cat [6]. However, it is difficult to compare the size of each produced cat as each experiment devised a different form of Schrödinger's cat living in a different system. Therefore, measures to quantify the size of macroscopic quantum superpositions have been proposed, which are sometimes called as "quantum macroscopicity" or "macroscopic quantumness." Nevertheless, as the measures have been developed from the experimental consideration or in empirical point of view rather than operational or axiomatic approaches as in entanglement measures, the meaning of each measure heavily depends on the context. Therefore,

the original problem of quantification is not solved; it is just moved to the problem of the measures. Then are these measures meaningless? Even though each measure quantifies the size of superposition using its own figure of merit, it is known that many of those measures reduce to the same form for pure states [7]. This implies that there may be some underlying physical principle which the measures can reveal. Therefore, it is worthwhile to investigate the properties and possible operational interpretations of the measure. These analyses would deepen our understanding and may guide us through the most general measure for quantum macroscopicity.

In this thesis, we conduct this analysis first. We first briefly review a proposed measure and investigate in what sense it can be related with macroscopic realism. The analysis firmly establishes the basis of the measure of quantum macroscopicity which will be used throughout the thesis. As a macroscopic superposition also follows from the superposition principle, it is also essential to compare quantum macroscopicity and entanglement to find the similarities and differences. We focus on many-particle spin-$1/2$ systems and use the geometric measure of entanglement as a measure of multipartite entanglement. This study shows that quantum macroscopicity measures a different quantity which mere entanglement cannot reveal. The application of quantum macroscopicity measure will be following to show that the macroscopic superpositions are rare in the Hilbert space of many-particle systems whereas geometric entanglement is commonly large. This result provides a kinematical point of view answer to the question why we cannot see macroscopic superpositions in the real world.

We further investigate the dynamics of a closed many-particle spin-$1/2$

system to address the question in dynamical point of view. We are able to show that macroscopic quantum superpositions disappear if a closed system dynamics yields thermalization. The result is compared with a system in many-body localization (MBL) phase which does not thermalize. Our study consistently shows that macroscopic superpositions are hard to be seen without assuming the openness of the system, which is one of the basic assumptions of decoherence theory [8].

The remaining chapters are summarized as follows. In Chapter 2, we introduce the measures for entanglement. We next show the definition of quantum macroscopicity and possible interpretations in Chapter 3. We compare these two type of quantum properties in Chapter 4 and investigate for random states ensembles in Chapter 5. We show the dynamics of quantum macroscopicity in a closed system in Chapter 6 and conclude with final remarks in Chapter 7.

Chapter 2

Entanglement in many-particle systems

In this chapter, we introduce two different entanglement measures for pure states. The first one is the entropy of entanglement for bipartite systems and the other one is the geometric measure of entanglement for multipartite systems. There are many other entanglement measures, especially in multipartite settings, but we just consider these two in this thesis as they have well-defined meaning and can be numerically calculated. Nevertheless, before going to the definitions of the measures, we briefly summarize the concept of entanglement and how it have been measured. They are crucial to understand how entanglement measures differ to quantum macroscopicity measures which we will introduce in the following chapter. The detailed definitions and the properties of general entanglement measures are beyond the scope of this thesis and the interested readers may find them in the review papers such as Refs. [9, 10, 11].

2.1 Introduction

Entanglement is one of the most widely investigated non-classical correlations which a quantum system can have. It is known that the term “entanglement” was first used by Schrödinger [12] and this term have been used to refer a non-separable quantum state. A separable state of a bipartite quantum system

(where each party is named A and B) is given as

$$\rho = \sum_i p_i \rho_A^{(i)} \otimes \rho_B^{(i)} \tag{2.1}$$

where $\rho_A^{(i)}$ and $\rho_B^{(i)}$ are any density matrices in the Hilbert space of A and B, respectively. As non-separable states obviously have a non-local correlation, it is used to be believed that any entangled state can violate local realism. Nevertheless, this was not the way nature works. In 1989, Werner revealed that there are some entangled states the outcome probabilities of which can be obtained using a local hidden variable [13]. After that, Popescu [14] and Peres [15] analyzed the violation of local realism under more general setups such as sequence of local generalized measurement, many copies of a quantum state, and post-selections. Entanglement in more general settings also have been investigated after it was known that many interesting non-classical operations such as quantum key distributions [16], quantum dense coding [17], and quantum teleportation [18] are possible using entanglement. These studies developed the methods to distill maximally entangled states from a general pure or mixed state only using local operations and classical communications (LOCCs) which are considered easy and classically feasible. The studies naturally induce entanglement measures called "distillable entanglement" and "entanglement of formation" which counts the number of maximally entangled states that can be obtained from or required to produce a given quantum state only using LOCCs [19, 20]. These entanglement measures have well-definite meanings. If a quantum state have distillable entanglement n/m, n maximally entangled states can be ob-

tained from the m copy of given state only using LOCCs. After distillation, we can use the resulting maximally entangled states to do a quantum task.

Even though the concept of theses measures is simple and have straightforward meanings, it is not easy to calculate the measures for general mixed states. Therefore, axiomatic entanglement measures were developed. In Ref. [21], the authors selected three specific properties of the previous entanglement measures to devise a different type of measure. They are (1) vanishing for separable states, (2) invariance under local unitary, and (3) non increasing under LOCC. In this sense, relative entropy of entanglement and logarithmic negativity were suggested as axiomatic entanglement measures. The above discussions to quantify entanglement using LOCC is called as "entanglement monotone" or "LOCC monotone." It generally assumes that LOCCs are free operations that we can do easily and do not cost quantum charges. It have been known that many of entanglement measures satisfying some assumptions reduce to the entanglement entropy for pure states which we introduce in the following section.

This framework have succeeded incredibly to quantify entanglement of bipartite systems, although, it is not simple to directly adjust this framework to multipartite cases. In bipartite case, we can uniquely define maximally entangled state up to local operations. For example, there are four orthogonal

maximally entangled states in a two-qubit system given as

$$|\Phi^{\pm}\rangle = \frac{1}{\sqrt{2}}(|0\rangle_A |0\rangle_B \pm |1\rangle_A |1\rangle_B) \tag{2.2}$$

$$|\Psi^{\pm}\rangle = \frac{1}{\sqrt{2}}(|0\rangle_A |1\rangle_B \pm |1\rangle_A |0\rangle_B). \tag{2.3}$$

which are also called as the Bell states. These four states are inter-convertible using local operations (applying X, Y, and Z gate locally to A part of $|\Phi^+\rangle$ generates all the other Bell states). Moreover, they can be transformed any bipartite pure states using LOCCs following Nielsen's theorem [22]. We cannot do this reversely, however; any pure state with smaller entanglement entropy cannot be transformed to a maximally entangled state by the LOCC monotone condition. Still, we can stochastically convert any entangled state of this system to a maximally entangled state with non-zero probability using LOCC. In this sense, Dür, Vidal, and Cirac first rigorously defined a class of entangled quantum states using stochastic LOCCs (SLOCCs) [23]. Under this definition, all entangled states in two-qubit systems are in the same class under SLOCCs. This is only for two-qubit systems, however. There are two distinct classes for the genuinely entangled states (not separable for any bipartition) for a system of three qubits. Specifically,

$$|W\rangle = \frac{1}{\sqrt{3}}(|0\rangle_A |0\rangle_B |1\rangle_C + |0\rangle_A |1\rangle_B |0\rangle_C + |1\rangle_A |0\rangle_B |0\rangle_C) \tag{2.4}$$

$$|\mathrm{GHZ}\rangle = \frac{1}{\sqrt{2}}(|0\rangle_A |0\rangle_B |0\rangle_C + |1\rangle_A |1\rangle_B |1\rangle_C) \tag{2.5}$$

are the W state and the GHZ (Greenberger-Horne-Zeilinger) state, respectively.

They are maximally entangled quantum states in each class so they cannot be transformed to each other with non-zero probability using SLOCCs. It means that we cannot order entangled states as in bipartite cases. In fact, each multipartite entanglement measure gives different ordering to $|W\rangle$ and $|\mathrm{GHZ}\rangle$. For example, 3-tangle and the geometric measure of entanglement are entanglement measures which satisfies LOCC monotone conditions (when defined for mixed states using convex-roof extension) but 3-tangle gives larger value for the GHZ state than the W state but the geometric entanglement gives the opposite ordering.

2.2 Entropy of entanglement

Then let us introduce the entropy of entanglement (or entanglement entropy in short) which is the most widely used measure for pure states in bipartite systems. We consider a bipartite system composed of two partitions A and B. The entanglement entropy for a bipartite pure state $|\psi\rangle_{AB}$ is given by

$$E_S(|\psi\rangle_{AB}) = -\operatorname{Tr}[\rho_A \log \rho_A]$$

where $\rho_A = \operatorname{Tr}_B[|\psi\rangle_{AB} \langle\psi|]$ is a reduced density matrix of $|\psi\rangle_{AB}$. Many entanglement measures such as distillable entanglement, entanglement cost, entanglement of formation, relative entropy of entanglement, and squashed entanglement reduce to the entanglement entropy for pure states. In fact, there is a general proof that a measure satisfying LOCC monotone conditions with several additional ones reduce to the entanglement entropy for pure states [24].

The eigenstate decomposition of a reduced density matrix ρ_A can be written as

$$\rho_A = \sum_{i=1}^{d_A} \lambda_i \left|\lambda_i\right\rangle \left\langle\lambda_i\right| \tag{2.6}$$

where d_A is the Hilbert space dimension of the subspace A and $\{\lambda_i\}$ are the eigenvalues of ρ_A and $|\lambda_i\rangle$ are the corresponding eigenvectors. Then entanglement entropy of this state is calculated as $E_S(|\psi_{AB}\rangle) = -\sum_i \lambda_i \log \lambda_i$. Specially, when the subsystems A and B have the same local dimension D, the bipartite state

$$|\psi_M\rangle = \frac{1}{\sqrt{D}} \sum_{i=1}^{D} |i,i\rangle_{AB} \tag{2.7}$$

gives the maximal value $S(|\psi_M\rangle) = \log D$. This state can be transformed any pure states in this system using only LOCC operations following Neilsen's theorem [22] so it is a maximally entangled state in this system.

Even though the entanglement entropy is a measure of entanglement for two party systems, it have been used to quantify entanglement of many-body systems. For these systems, we divide the whole system which can be finite or infinite into two parties A and B where A is a concatenated region and B is the rest of the system. For example, entanglement area law [25] is formulated using the entanglement entropy which says that the ground state of the Hamiltonian for usual many-body systems has entanglement entropy proportional to the boundary of A.

Finally, we note that the entanglement entropy can be numerically calculated after diagonalizing the reduced density matrix ρ_A from the definition. Diagonalization of $D \times D$ matrices usually consumes $\mathcal{O}(D^3)$ times and modern personal computers can calculate this very fast (within a second) for $D < 10^3$ matrices.

2.3 Geometric measure of entanglement

Geometric measure of entanglement (or geometric entanglement in short) is a measure which quantifies the entanglement of multipartite quantum systems. It is defined via the maximal overlap between the given state with any separable state $|\Phi\rangle_{\text{sep}} = |\phi_1, \phi_2, \cdots, \phi_N\rangle$,

$$E_G(|\psi\rangle) = -\log_2 \sup_{|\Phi_{\text{sep}}\rangle} |\langle\psi|\Phi_{\text{sep}}\rangle|^2. \tag{2.8}$$

Geometric entanglement E_G is bounded above by $N-1$ for N qubits (N spin-$1/2$ particles) and vanishes for separable states. Large value of the geometric entanglement is commensurate with the a large value of generalized Schmidt measure [26] which means that the large number of product states are needed to express the state.

In addition, it is known that we can make a measure for general mixed states satisfying LOCC monotone conditions by extending it using the convex roof construction [27, 28].

The geometric entanglement is also widely used for many-body systems. If a ground state is translational symmetric, an ansatz for a closest product

state $|\phi\rangle^N$ is usually used to calculate the measure (however, this ansatz can be failed. See Ref. [29] for details). Nevertheless, numerical calculations of the measure for general many-particle systems are not easy as we will see in the following.

2.3.1 Numerical calculation of geometric entanglement

Numerical computation of geometric entanglement is not easy for general quantum states as we do not know the basis of the closest separable state. In fact, to directly calculate the supremum in Eq. (2.8), we have to solve a very massive optimization problem. A general separable state for N qubits is parametrized using $2N$ real parameters $(x_1, x_2, \cdots, x_N)$ and $(y_1, y_2, \cdots, y_N)$ as

$$|\Psi_{\text{sep}}\rangle = \otimes_{i=1}^{N}(\cos x_i\,|0\rangle + e^{iy_i}\sin x_i\,|1\rangle). \tag{2.9}$$

As an optimization problem involving $2N$ parameters is usually NP-hard, directly solving Eq. (2.8) requires significant computational expenses as N increases.

Instead, a method to find the closest separable state using stochastic iterations has suggested in Ref. [30]. We here briefly introduce this algorithm. Suppose that we want to obtain the closest states to a three-qubit state $|\psi\rangle$. We first choose a random product state $|\phi_0\rangle = |0_0^1\rangle\,|0_0^2\rangle\,|0_0^3\rangle$ where the upper index denotes the party and the lower index indicates the number of step. Then, we calculate $|\tilde{\psi}\rangle = (\langle 0_0^2|\,\langle 0_0^3|)\,|\psi\rangle$ which is not normalized. If we replace $|0_0^1\rangle$ with

$|0_1^1\rangle = |\tilde{\psi}\rangle / \sqrt{\langle\tilde{\psi}|\tilde{\psi}\rangle}$ from $|\phi_0\rangle$, the resulting state $|0_1^1\rangle\,|0_0^2\rangle\,|0_0^3\rangle$ is the closest state to $|\psi\rangle$ for given two-qubit state $|0_0^2\rangle\,|0_0^3\rangle$. We next do the same procedure for the second qubit by first calculating $(\langle 0_1^1|\,\langle 0_0^3|)\,|\psi\rangle$ and normalize it and replace $|0_0^2\rangle$. The resulting state is named $|0_1^2\rangle$. After doing this for the third qubit, we finish the first step and obtain the resulting state $|\phi_1\rangle = |0_1^1\rangle\,|0_1^2\rangle\,|0_1^3\rangle$. We obtain the state $|\phi_n\rangle = |0_n^1\rangle\,|0_n^2\rangle\,|0_n^3\rangle$ after repeating this step for n times which would be a approximated solution of the closest state. This scheme actually splits the whole optimization problem to local optimizations.

However, what this algorithm actually does is the generalized Schmidt decomposition but not finding the closest state. As the generalized Schmidt decomposition is not unique, the resulting state depends on the initial choice $|\psi_0\rangle$. Therefore, it is not guaranteed that the state $\lim_{n\to\infty}|\phi_n\rangle$ is the optimal state for Eq. (2.8). In practical case, by repeating the whole algorithm for many randomly chosen initial states, a close approximated value of the geometric entanglement is found. Still, as the inner product required to calculate $|0_n^k\rangle$ consumes $\mathcal{O}(2^N)$ operations, this algorithm does not give an exponential speed up.

Chapter 3

Measure for quantum macroscopicity

In this chapter, we define a measure for the size of macroscopic quantum superpositions which is usually called as "quantum macroscopicity" or "macroscopic quantumness" and investigate the properties and operational meanings of it. There are some different measures for general mixed states in many-particle spin-$1/2$ systems, and we do not know which one is better than the others. Yet, as they all give the same value for pure states, we here mainly focus on the measure for pure states and investigate its properties.

However, before going to the definition of our measure, we introduce a brief history of the attempts to quantify the size of macroscopic superpositions because it helps to understand how the measures have been developed over the years and why this problem is interesting. More detailed review about the measures can be found in Ref. [31].

3.1 Historical introduction

After quantum theory of superfluidity and superconductivity had developed, some people said that they are the apparent signatures of the validity of quantum mechanics in macroscopic systems. However, Leggett in 1980 argued in his seminal paper that such phenomena are just by the accumulation microscopic quantum effects but not really test quantum mechanics in macro-

scopic scale [32]. He also argued that an observation of a superposition between *macroscopically distinct* objects, which is originally illustrated in the Schrödinger's Cat paradox, is necessary to test quantum mechanics in macroscopic scale. He also presented the first measure named "disconnectivity" D which tests whether a quantum state is a macroscopic superposition or not and suggested a possible experiment to implement a macroscopic superposition using a superconducting device. Even though the measure D captures some property of a macroscopic superposition, there are some limitations in this measure. The measure D does not well order the states the sizes of which are apparently different and not properly operate for mixed states [31].

However, the measure itself had not been a special issue over the two decades. It was the year 2002 when the problem about the size of superposition is rediscovered by Dür et. al. [33] after the several experiments to make a macroscopic superposition [34, 35] was successfully done in superconducting quantum interference device (SQUID). Using a well developed technique in quantum information theory, the authors investigated the effective size of macroscopic superposition of the form $|\psi\rangle = |\phi_1\rangle^{\otimes N} + |\phi_2\rangle^{\otimes N}$ when $|\phi_1\rangle$ and $|\phi_2\rangle$ are two non-orthogonal sates of qubit (or two-level system, equivalently) with $|\langle\phi_1|\psi_2\rangle|^2 = 1 - \epsilon^2$. They investigated two different quantities. The first one is the speed of decay of the coherence terms under dephasing noise and the second one is how large n qubit GHZ state $|\mathrm{GHZ}\rangle_n = |0\rangle^{\otimes n} + |1\rangle^{\otimes n}$, which is considered as the maximum macroscopic superposition, can be distilled from $|\psi\rangle$ using LOCCs in asymptotic setting. Both quantities give the same effective size of superposition for $|\psi\rangle$ that turns out to be $N\epsilon^2$ assuming $\epsilon \ll 1$, where

we set the size of N qubit GHZ state as N.

Parallelly, Shimizu and Miyadera investigated a similar problem but in a different motivation [36]. They investigated the fragility of a pure quantum state in many-body systems and showed that it is related with the cluster property which the infinite system should have. The cluster property arises when we construct the Hilbert space of an infinite lattice system and can be used to explain the spontaneous symmetry breaking of a quantum system [37, 38]. This property assert that a quantum state in an infinite length system cannot have a correlation between two infinitely separated sites. From this property, they deduced that a quantum state $|\psi\rangle$ which has the quantum fluctuation $\langle\psi|(\Delta A)^2|\psi\rangle = \Theta(N^2)$[1] can exist only in a finite system and regarded these states as macroscopic superpositions. In thermodynamic limit where $N \to \infty$, this state cannot preserve the superposition by the cluster property and changes to classical mixture. Here, N represents the size of whole system, $A = \sum_{x\in X} a(x)$ is any possible summation of local observables where we introduce X to represent the whole system with $|X| = N$ and $\Delta A = A - \langle\psi|A|\psi\rangle$. In addition, they argued that the variance of A is related to the decay rate of the coherence (quantified using the purity) when the system is coupled to an external bath therefore such states are fragile even for a finite system.

For example, let us consider the GHZ state in N qubit system which is written by $|\mathrm{GHZ}\rangle_N = |0\rangle^{\otimes N} + |1\rangle^{\otimes N}$. This state has the fluctuation $\langle\psi|(\Delta S_z)^2|\psi\rangle = N^2$ when $S_z = \sum_i \sigma_z^i$ is a total spin-z operator. The cluster property say that in $N \to \infty$, the GHZ state will be a incoherent

[1] Big-O and big-Θ notations are summarized in Appendix A.

mixture between two component states given by $|0\rangle\langle 0|^{\otimes N} + |1\rangle\langle 1|^{\otimes N}$. This is actually the way we explain the spontaneous symmetry breaking of the ground state of the Ising model the Hamiltonian of which is given by $H = \sum_i \sigma_z^i \sigma_z^{i+1}$ [38]. Moreover, coupling to an external bosonic bath with a Hamiltonain $H_{SB} = \hat{a}S_z + (h.c.)$ induces decoherence of the system where the purity decay rate at $t = 0$ is given by $\langle\psi|(\Delta S_z)^2|\psi\rangle = N^2$.

Even though well defined problems and operational interpretations, these studies have some restrictions and their approaches are not easily generalized. First, Dür et al. only considered a superposition between two product states. As their quantification of the fragility is based on the decay rate of the off diagonal term, it cannot be directly applied to multi-component superpositions. For example, it is not easy to investigate the fragility of $|00\cdots0\rangle + |10\cdots0\rangle + |11\cdots0\rangle + \cdots + |11\cdots1\rangle$ as the dephasing rates of each off-diagonal term are different. Investigating the rate of LOCC distillation to the GHZ state is much more difficult. A general distillation scheme of multipartite states is not known. Only a LOCC transformation scheme for GHZ entanglement cost (the opposite way) is recently known [39] and it is generally believed that finding a distillation scheme is harder than that of a cost scheme [40]. Therefore, it is not easy to apply their methods to calculate the size of a general quantum state.

On the other hand, the work by Shimizu and Miyadera just proposed a criterion of macroscopic superposition. The criterion was also extended to general mixed states [41] but these works just discriminate macroscopic superposed quantum states and the others and do not provide a quantification of the size for macroscopic superposition.

There had been several other attempts [42, 43, 44, 45] to devise a measure for the size of macroscopic superpositions but they suffer similar problems as they restrict a specific form of quantum states or just proposed a criterion. It was in 2011 that Lee and Jeong [46] devised a general measure applicable to any form bosonic quantum states including mixed and multipartite states. The measure by Lee and Jeong has some clear meanings. It quantifies the fringes in the phase space and the value of it is the same to the purity decay rate under the dissipative Lindbladian coupling with an environment.

After that, general measures for many-particle spin systems also have been proposed. Fröwis and Dür suggested maximum quantum Fisher information over the collective observables as a general measure for quantum macroscopicity [47]. Another measure for such systems is also proposed recently by the author and colleagues from the same concept of Lee and Jeong measure [48].

It is interesting that both measures appear in Refs. [47, 48] for many-particle spin systems reduce to the same form (maximum variance of local additive spin operators) for pure states, which has used by Shimizu and Miyadera. Moreover, Fröwis et al. showed that many of the proposed measures for bosonic systems also can be transformed into the same form by photon-spin mapping [7]. We will discuss the detailed definition and properties of this measure in the following section.

We here note that the history of quantum macroscopicity is very different to that of entanglement measures introduced in the previous chapter. Measures have been developed following experiments and in empirical ways rather than theory driven. This is not only the difference between two. Entanglement mea-

sures usually have clear meanings. For example, if a quantum state have a non-vanishing distillable entanglement then we can use many of such states and LOCCs to distill the maximally entangled states and can violate local realism using the distilled state. In contrast, the relation between quantum macroscopicity measures and macroscopic realism [4, 49] is vague. Moreover, we still do not have a resource theoretic approach to this measure. This may because it is difficult to answer what operations are classical in the sense of macroscopic realism in the same way to LOCC which can be considered classical in the sense of local realism.

Recently, there have been some progresses to address these questions. A coarse-grained measurement which is a measurement with a finite precision [50, 51] have recently considered as a possible bridge that can relate a measure of quantum macroscopicity to macroscopic realism [52, 53, 54]. We take a look these argument briefly in the following section. An axiomatic approach to quantum macroscopicity measure has also recently proposed [55]. Though, this study does not answer to the fundamental question that what is a macroscopic quantum superposition; it just restate axiomatic conditions of asymmetry measures [56, 57]. How the properties of asymmetric measure can be related to quantum behaviors in macroscopic scale is a more big problem which need to be addressed. For instance, a study by Kwon et al. [54] suggests a counterexample that shows the insufficiency of theses conditions for a measure of quantum macroscopicity.

In summary, even though there have been a lot of efforts to devise a general quantum macroscopicity measure, we still have many interesting open

questions.

3.2 Definition and properties

We here consider a pure quantum state of N-particle spin-$1/2$ system. The measures introduced in Ref. [36] is given as

$$\mathcal{M}(|\psi\rangle) = \max_{A \in S} \mathcal{V}_A(|\psi\rangle) \tag{3.1}$$

where

$$\mathcal{V}_A(|\psi\rangle) = \left[\langle\psi|A^2|\psi\rangle - \langle\psi|A|\psi\rangle^2\right] \tag{3.2}$$

is the variance of A for a given state $|\psi\rangle$. The set of observable S is given as

$$S = \left\{ \sum_{i=1}^{N} \vec{\alpha}_i \cdot \boldsymbol{\sigma}^{(i)} : |\vec{\alpha}_i| = 1 \right\} \tag{3.3}$$

where $\boldsymbol{\sigma}^{(i)} = \{\sigma_x^{(i)}, \sigma_y^{(i)}, \sigma_z^{(i)}\}$ is a vector of Pauli operators for i-th particle. An operator in S is commonly called as "collective observables" but "local-additive observables" [36] or "macroscopic observables" [58] is also used. The measures introduced in Refs. [47, 48] reduces to the same form for pure states and different quantum macroscopicity meausres for bosonic systems are also related to this form [7]. In addition, recent proposed axiomatic approach shows that this can be a measure satisfying several axiomatic constraints [55].

As the measure $\mathcal{M}$ gives the minimum value N and the maximum value

N^2 (see the following section), we also define the normalized version of it as

$$\mathcal{I}(|\psi\rangle) = \mathcal{M}(|\psi\rangle)/N. \tag{3.4}$$

As the scaling behavior of quantum macroscopicity is better captured by $\mathcal{I}$, we will use $\mathcal{I}$ more often than $\mathcal{M}$ in the following chapters.

From the definition, a lower and upper bounds of the measure are given as

$$1 \leq \mathcal{I}(|\psi\rangle) \leq N. \tag{3.5}$$

The equality in the upper bound is satisfied if and only if $|\psi\rangle$ is equivalent to the GHZ-state up to local unitary matrices, i.e., $|\psi\rangle = U_1 \otimes \cdots \otimes U_N \, |\mathrm{GHZ}\rangle_N$ where each U_i is a 2×2 unitary matrix. In addition, if $|\psi\rangle$ is a product state, $\mathcal{I}(|\psi\rangle) = 1$. Note that this is not the if and only if condition. There are some entanglement states $|\psi\rangle$ which give $\mathcal{I}(|\psi\rangle) = 1$ (see the following Chapter for details).

References [36, 47, 48] provide interpretations of scaling behaviors for a class of quantum states. Let us consider a class of quantum states $\{|\psi\rangle_N\}$ where each $|\psi\rangle_N$ is a quantum state defined for a N-particle spin system. Then the studies suggest that if $\mathcal{M}(|\psi\rangle_N) = \mathcal{O}(N)$, or equivalently $\mathcal{I}(|\psi\rangle_N) = \mathcal{O}(1)$, then $|\psi\rangle_N$ is not a macroscopic superposition whereas $\mathcal{M}(|\psi\rangle_N) = \Theta(N^2)$ ($\mathcal{I}(|\psi\rangle) = \Theta(N)$) means $|\psi\rangle_N$ is a macroscopic superposition. The argument is based on the fragility of quantum states when it is interacting to a bath [36, 48] or the improvement of precise measurements [47]. Another supporting arguments are presented in Refs. [52, 53] based on coarse-grained measurements

scheme [50, 51]. As they directly connect the measure for quantum macroscopicity and macroscopic realism, we discuss about these arguments in the next section.

We finalize this section after briefly mention about quantum macroscopicity measure for bosonic systems. Historically, a general measure for quantum macroscopicity (including mixed and any kind of superpositions) first appeared for bosonic states by Lee and Jeong [46]. The measure introduced by the authors for a general mixed state ρ is defined as

$$\mathcal{M}_{LJ}(\rho) = \sum_{i=1}^{N} \mathrm{Tr}\left[\rho^2 a_i^\dagger a_i - \rho a_i \rho a_i^\dagger\right] \tag{3.6}$$

where each a_i and $a_i^\dagger$ are annihilation and creation operators for i-th bosonic mode, respectively, and satisfying $[a_i, a_i^\dagger] = 1$. However, this definition of measure does not capture the correlation between modes (macroscopicity distributed among several modes [7, 55]). Therefore, like the measure for spin systems, a modified definition

$$\mathcal{M}_b(|\psi\rangle) = \max_{A \in T} \mathcal{V}_A(|\psi\rangle) \tag{3.7}$$

has been used for pure states in bosonic systems [55, 59]. Here, the set of measurement operators T is given as

$$T = \left\{ \sum_{i=1}^{N} x_i^{\theta_i} : \theta_i \in [0, 2\pi) \right\} \tag{3.8}$$

where each $x_i^{\theta_i} = (a e^{i\theta_i} + a^\dagger e^{-i\theta_i})/\sqrt{2}$ is a quadrature operator for mode i. We

note that for a single mode pure bosonic state, the measure $\mathcal{M}_{LJ}$ (Eq. (3.6)) reduces to $[\mathcal{V}_x(|\psi\rangle) + \mathcal{V}_p(|\psi\rangle) - 1]/2$ where x and p are quadrature operators with $\theta = 0$ and $\pi/2$, respectively. This form directly relates $\mathcal{M}_{LJ}$ and $\mathcal{M}_b$ (Eq. (3.7)).

3.3 Measure of quantum macroscopicity and coarse-grained measurement

A coarse-grained measurement is a measurement operator with a finite precision. These measurements are regraded classical as it enables the measurements without disturbance of quantum states and may recover macroscopic realism for pure states. Moreover, the classical concept of distance enters in this type of measurement.

To understand the relation between coarse-grained measurements and quantum macroscopicity, we recall the following obvious fact: Any orthogonal states can be discriminated by quantum measurements. For example, in quantum mechanics, we can consider the set of projective measurement operators $\{|\psi\rangle\langle\psi|, \mathbb{1} - |\psi\rangle\langle\psi|\}$ for some quantum state $|\psi\rangle$. However, this measurement is quantum in the sense that it can discriminate any small superposition (microscopic superposition). For example, component states $|0\rangle$ and $|1\rangle$ in the superposition $|0\rangle + |1\rangle$ are distinguished for $|\psi\rangle = |0\rangle$. Likewise, component states of the superposition $|0000\rangle + |0001\rangle$ as well as $|0000\rangle + |1111\rangle$ also can be distinguished. The above argument says that there is no concept of "macroscopically distinct" in quantum mechanics:

Every orthogonal states are distinct. Consistent with our observation, this measurement is sufficient to violate macroscopic realism [50].

Then how can we add the concept of "macroscopically distinct" in quantum mechanics? We first need an observable the eigenvalues of which have a classical meaning [60]. For example, for a spin-J system, an observable J_z measures z-component of spin that may be regarded classical. The eigenvalues are directly connected to the size of magnetism which is also in classical physics. For this observable, we consider the eigenstates with a small difference between corresponding eigenvalues as "close", but with a large difference as "far". For example, $|J_z = 20\rangle$ and $|J_z = 21\rangle$ may be regarded as close but $|J_z = -20\rangle$ and $|J_z = 20\rangle$ as far for $J = 25$ spin system under our consideration. Moreover, it is reasonable to assume that our measurement apparatuses cannot discriminate all eigenvalues for real macroscopic system, e.g. $J \gg 1$. In other words, they have a finite resolution Δ (cannot discriminate nearby Δ eigenvalues). Then this measurement can be regarded as a coarse-grained type [50] and can discriminate "macroscopically distinct" state.

It is known that coarse-grained measurements that do not disturb a coherent state (the most classical-like state among all pure states) may recover classical outcome probabilities [58, 50]. In our example, $\Delta \gg \sqrt{J}$ is such condition. However, the assumption of coarse-grained measurements alone is not sufficient for macroscopic realism. When a Hamiltonian of the system generates a quantum state which can give several different measurement outcomes under a coarse-grained measurement of this resolution [51] or certain quantum state is disturbed by a coarse-grained measurement then macroscopic re-

alism can be violated (no-signaling in time in general [49]). In this sense, we may define a macroscopic quantum superposition as a state that can violate macroscopic-realism under coarse-grained measurement.

Under this definition, it is possible to investigate a macroscopic quantum superposition in a N-particle spin-$1/2$ system. First, assume that we measure an observable A in the set S (Eq. (3.3)). It is also simple to assume that our coarse-grained version of A smears the eigenvalues in Gaussian weight. Then for eigenvalue decomposition $A = \sum_i a_i \left|i\right\rangle \left\langle i\right|$, the set of Kraus operators for coarse-grained version of A is given by

$$Q^{\Delta}(x) = \sum_i \sqrt{q_i^{\Delta}(x)} \left|i\right\rangle \left\langle i\right| \tag{3.9}$$

where $q_i^{\Delta}(x) = (\sqrt{2\pi}\Delta)^{-1} \exp[-(a_i - x)^2/(2\Delta^2)]$. It is easy to check that they are valid Kraus operators as $\int dx\, Q^{\Delta}(x)^{\dagger} Q^{\Delta}(x) = \mathbb{1}$.

For this coarse-grained version of A, the following results have obtained [58, 54]

$$\sqrt{\mathcal{F}(\left|\psi\right\rangle, \Phi_{\Delta}(\left|\psi\right\rangle \left\langle\psi\right|))} \geq \exp\Big[-\frac{\mathcal{V}_A(\left|\psi\right\rangle)}{4\Delta^2}\Big] \tag{3.10}$$

where $\mathcal{F}(\left|\psi\right\rangle, \rho)) = \left\langle\psi\right|\rho\left|\psi\right\rangle|^2$ is the fidelity between a pure quantum state $\left|\psi\right\rangle$ and a mixed state ρ and $\Phi_{\Delta}(\left|\psi\right\rangle \left\langle\psi\right|) = \int dx\, Q^{\Delta}(x) \left|\psi\right\rangle \left\langle\psi\right| Q^{\Delta}(x)^{\dagger}$ is a quantum state after the coarse-grained measurement.

The most classical states in our system is a spin coherent state $\left|\phi\right\rangle^{\otimes N}$ where $\left|\phi\right\rangle = a\left|0\right\rangle + b\left|1\right\rangle$ is any spin-$1/2$ state. As $\mathcal{M}(\left|\phi\right\rangle^{\otimes N}) = \max_{A\in S} \mathcal{V}_A(\left|\phi\right\rangle^{\otimes N}) = N$, $\Delta \gg \sqrt{N}$ is a sufficient condition for not disturb-

ing a spin coherent state for any $A \in S$. Moreover, all quantum states that have $\mathcal{M} = O(N)$ are not disturbed by coarse-grained measurement for this value of Δ. Therefore, we can consider that such states are not a macroscopic superposition. On the other hands, if a quantum state $|\psi\rangle$ gives $\mathcal{M} > O(N)$, $|\psi\rangle$ can be disturbed by some coarse grained version of $A \in S$ even though the measurement do not disturb a spin coherent state. Therefore, such a state can be regarded as a macroscopic superposition.

3.4 Numerical methods to calculate quantum macroscopicity

Numerical calculation of the quantum macroscopicity measure $\mathcal{M}$ requires optimization of the directions $\{\vec{\alpha}_i\}$ in Eq. (3.1). As two real numbers are required to parametrize each $\vec{\alpha}_i$, we need to solve an optimization problem of $2N$ variables as in geometric entanglement to evaluate the value of measure.

However, there is a more efficient way to evaluate $\mathcal{M}(|\psi\rangle)$. First, we can reduce the calculation time to obtain the variance $\mathcal{V}_A = \langle\psi|A^2|\psi\rangle - \langle\psi|A|\psi\rangle^2$ after decomposing A into components. If we directly evaluate this after constructing $A \in S$ using $2N$ parameters, it requires large numerical efforts as A is a $2^N \times 2^N$ (sparse) matrix. However, after denoting the components of $\vec{\alpha}_i = \{\vec{\alpha}_{i,x}, \vec{\alpha}_{i,y}, \vec{\alpha}_{i,z}\}$ we can express the variance of A as

$$\langle\psi|A^2|\psi\rangle - \langle\psi|A|\psi\rangle^2 = \sum_{i,j=1}^{N} \sum_{a,b\in\{x,y,z\}} \alpha_{i,a}\alpha_{j,b} \tag{3.11}$$

$$\times \left[\langle\psi|\sigma_a^{(i)}\sigma_b^{(j)}|\psi\rangle - \langle\psi|\sigma_a^{(i)}|\psi\rangle \langle\psi|\sigma_b^{(j)}|\psi\rangle\right]. \tag{3.12}$$

We then first construct a $3N \times 3N$ matrix $W_{ia,jb}$ for the given quantum state $|\psi\rangle$ as

$$W_{ia,jb} = \langle\psi|\sigma_a^{(i)}\sigma_b^{(j)}|\psi\rangle - \langle\psi|\sigma_a^{(i)}|\psi\rangle \langle\psi|\sigma_b^{(j)}|\psi\rangle \tag{3.13}$$

and calculate $\langle\psi|A^2|\psi\rangle - \langle\psi|A|\psi\rangle^2$ using this matrix as

$$\langle\psi|A^2|\psi\rangle - \langle\psi|A|\psi\rangle^2 = \langle\boldsymbol{\alpha}, W\boldsymbol{\alpha}\rangle \tag{3.14}$$

where $\boldsymbol{\alpha} = \{\alpha_{1,x}, \alpha_{1,y}, \alpha_{1,z}, \alpha_{2,x}, \cdots, \alpha_{N,z}\}$ is a vector of $3N$ components and $\langle\cdot,\cdot\rangle$ is the inner product between two vectors. In practice, it is convenient to use a symmetric version of W defined as

$$V = \frac{W + W^T}{2} \tag{3.15}$$

because V is a real matrix in this construction. The matrix V is usually called as the variance-covariance matrix (VCM) and have been used in several previous studies [61, 62] to efficiently calculate the variances. Then the calculation of Eq. (3.1) is to solve the optimization problem

$$\begin{aligned} &\underset{\boldsymbol{\alpha}}{\text{maximize}} \quad \langle\boldsymbol{\alpha}, V\boldsymbol{\alpha}\rangle \\ &\text{subject to} \quad |\vec{\alpha}_i| = 1,\ i = 1, \ldots, N. \end{aligned} \tag{3.16}$$

This optimization problem is a quadratically constrained quadratic program which is generally NP-hard as NP-hard 0-1 integer programming can be converted into this form. As the number of optimizing variables is $3N$ and

the number of constraints is N for our problem, it is expected that more than exponential time of N is required to obtain the complete solution of the optimization problem. Nevertheless, typical numerical optimization problems including ours only require *practically approvable* solutions not the complete solutions. Many algorithms for function optimization are known to give a such feasible solution in a polynomial time of N for this problem. The Broyden–Fletcher–Goldfarb–Shanno (BFGS) method [63] which will be used throughout the thesis is a good example. Therefore, even though the number of parameters for the optimization of this problem is the same to the geometric entanglement case, we can calculate quantum macroscopicity measure more quickly.

In addition, an upper bound of the optimized value is given by

$$\mathcal{M}(|\psi\rangle) \leq N\lambda_1 \tag{3.17}$$

where λ_1 is the largest eigenvalue of V. This is because the value $N\lambda_1$ is the solution of the optimization problem when the constraints are loosen to $|\boldsymbol{\alpha}| = \sum_i |\vec{\alpha}_i|^2 = N$. In this case, choosing $\boldsymbol{\alpha}$ as the eigenstate of V with the eigenvalue λ_1 give the solution.

The optimization problem is readily simplified if a quantum state $|\psi\rangle$ is

permutation symmetric. In this case, the matrix V is given as

$$V = \begin{pmatrix} B & C & \dots & C \\ C & B & \dots & C \\ \vdots & \vdots & \ddots & \vdots \\ C & C & \dots & B \end{pmatrix} \tag{3.18}$$

where the components of 3×3 matrices B and C are given as $B_{a,b} = \delta_{a,b} - \langle\psi|\sigma_a|\psi\rangle \langle\psi|\sigma_b|\psi\rangle$ and $C_{a,b} = \langle\psi|\sigma_a \otimes \sigma_b|\psi\rangle - \langle\psi|\sigma_a|\psi\rangle \langle\psi|\sigma_b|\psi\rangle$. We here dropped the indices of spin sites as the state is permutation symmetric. Then it is simple to show that $\mathcal{M}(|\psi\rangle) = N\lambda_1$ where λ_1 is the largest eigenvalue of V. First, note the upper bound Eq. (3.17) and the eigenvalues of V are also the eigenvalues of $B + (N-1)C$. Then, let the corresponding eigenvector of $B + (N-1)C$ with the eigenvalue λ_1 be $\vec{\alpha}$. Without loss of generality, we can normalize the vector as $|\vec{\alpha}| = 1$. Then it is directly obtained that $\vec{\alpha}_i = \vec{\alpha}$ for all i gives $\langle \boldsymbol{\alpha}, V\boldsymbol{\alpha}\rangle = N\lambda_1$. Therefore, $\mathcal{M}(|\psi\rangle) = N\lambda_1$ is obtained for a permutation symmetric state $|\psi\rangle$ which only requires the diagonalization of 3×3 matrix $B + (N-1)C$.

Chapter 4

Comparison between quantum macroscopicity and entanglement[1]

In the previous chapters, we have introduced two different type of quantumness for many-particle systems, entanglement and quantum macroscopicity. We now want to know how they are related and how much they are different.

In this chapter, we first provide an intuitive picture using a bosonic state usually called as the optical cat state. This example shows that quantum macroscopicity increases unboundedly even for finite entanglement, which implies that two concepts are not just simply connected.

We more strictly investigate the relations using N-particle spin-$1/2$ systems which we mainly concern in this thesis. We explicitly compare geometric entanglement and quantum macroscopicity for different types of quantum states living in this system. Actually, Ref. [65] performed a similar comparison where the author states that "a state which includes superposition of macroscopically distinct states also has large multipartite entanglement in terms of the distance-like measures of entanglement." We partially confirm and refuse this statement. We first show that geometric entanglement is indeed necessary for non-vanishing quantum macroscopicity. However, more complicated structure is found after extensive investigations. For instance, there are some entan-

[1]The contents of this chapter is largely based on the first part of Ref. [64]

gled states with strictly vanishing quantum macroscopicity. More surprisingly, we also find that very large value of geometric entanglement is a negative signature for quantum macroscopicity. As a consequence, the two quantities present different kinds of quantumness and cannot be used as synonymous.

4.1 Entanglement versus quantum macroscopicity for optical cat state

We here consider the optical cat states represented as

$$|\mathrm{C}_{\alpha}^{\pm}\rangle = \mathcal{N}_{\alpha}^{\pm}(|\alpha\rangle \pm |-\alpha\rangle) \tag{4.1}$$

where $|\alpha\rangle = D(\alpha)\,|0\rangle$, $D(\alpha) = \exp(\alpha a^{\dagger} - \alpha^{*} a)$ is a displacement operator and $\mathcal{N}_{\alpha}^{\pm} = 1/\sqrt{2 \pm 2e^{-2|\alpha|^2}}$ is a normalization constant. As $|\mathrm{C}_{\alpha}^{\pm}\rangle$ is a single mode state, we cannot define an entanglement. However, for optical state, we can easily do a beam splitter operation. After transmitting a 50:50 beam splitter, we get a state

$$|\mathrm{ECS}_{\alpha}^{\pm}\rangle = \mathcal{N}_{\alpha}^{\pm}(|\alpha/\sqrt{2}\rangle \otimes |\alpha/\sqrt{2}\rangle \pm |-\alpha/\sqrt{2}\rangle \otimes |-\alpha/\sqrt{2}\rangle) \tag{4.2}$$

which is usually referred as an entangled coherent state.

Quantum macroscopicity $\mathcal{M}_b$ (Eq. (3.7)) for this state can be easily calculate. We here focus on $|\mathrm{ECS}_{\alpha}^{+}\rangle$ quantum macroscopicity of which is given by $\mathcal{M}_b(|\mathrm{ECS}_{\alpha}^{+}\rangle) = 2|\alpha|^2/(1 + e^{-2|\alpha|^2}) + 1/2$ which is the same to $\mathcal{M}_b(|\mathrm{C}_{\alpha}^{+}\rangle)$. For large value of $\alpha \gg 1$, $\mathcal{M}_b \propto 2|\alpha|^2$ which means unbounded growth of

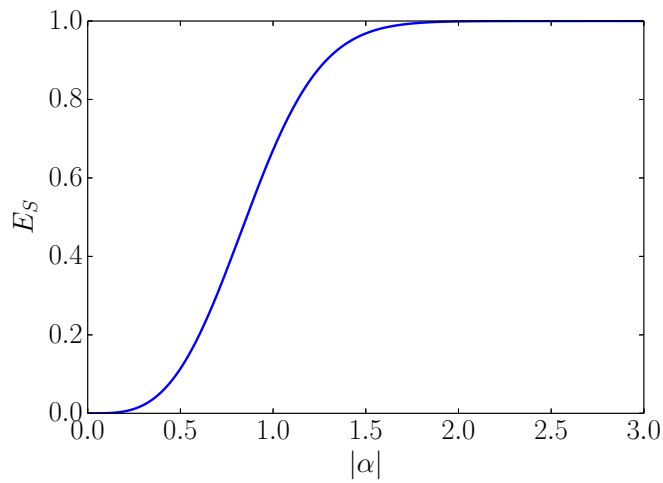

Figure 1: Entanglement entropy as a function of the amplitude of coherent state $|\alpha|$ for an entangled coherent state $|\mathrm{ECS}^+_\alpha\rangle$. It monotonically increases to 1 as $|\alpha|$ increases.

quantum macroscopicity with $|\alpha|$.

The behavior of the entanglement entropy is contrasting. A quantum state $|\mathrm{ECS}^\pm_\alpha\rangle$ lives in the Hilbert space $\mathbb{C}^2 \otimes \mathbb{C}^2$ that limits the maximal value of entanglement entropy to 1. For example, using the orthogonal basis generated by $\{|C^+_{\alpha/\sqrt{2}}\rangle, |C^-_{\alpha/\sqrt{2}}\rangle\}^{\otimes 2}$, $|\mathrm{ECS}^+_\alpha\rangle$ is represented as

$$|\mathrm{ECS}^+_\alpha\rangle = \frac{\mathcal{N}^+_\alpha}{2(\mathcal{N}^+_{\alpha/\sqrt{2}})^2}\,|C^+_{\alpha/\sqrt{2}}\rangle \otimes |C^+_{\alpha/\sqrt{2}}\rangle + \frac{\mathcal{N}^+_\alpha}{2(\mathcal{N}^-_{\alpha/\sqrt{2}})^2}\,|C^-_{\alpha/\sqrt{2}}\rangle \otimes |C^-_{\alpha/\sqrt{2}}\rangle\,. \tag{4.3}$$

It is easy to show that the state becomes a maximally entangle state in this subspace in the limit of $|\alpha| \to \infty$. Using this representation, we can easily calculate the entanglement entropy and plot the result as a function of amplitude $|\alpha|$ in Fig. 1. It shows monotonic increasing behavior with $|\alpha|$ and is bounded

above by 1. This example directly shows that entanglement is different to quantum macroscopicity in general. We reveal more strict relation between entanglement and quantum macroscopicity in the next section using many-particle spin systems.

4.2 Entanglement versus quantum macroscopicity for spin systems

4.2.1 Close-to-separable states

We first consider a quantum state $|\psi\rangle$ the maximal overlap between a separable state η is larger than or equal to 1/2, i.e. the geometric measure of entanglement $E_G(|\psi\rangle)$ [Eq. (2.8)] is smaller than or equal to unity.

Generalized GHZ states $|\Xi(\theta,\epsilon)\rangle$ which are given as the superpositions between two product states $|0\cdots0\rangle$ and $(\cos\epsilon\,|0\rangle+\sin\epsilon\,|1\rangle)^{\otimes N}$ with different weight are usually used to investigate quantum macroscopicity. Formally, it can be written as

$$|\Xi(\theta,\epsilon)\rangle=\frac{\cos\theta\,|0\rangle^{\otimes N}+\sin\theta(\cos\epsilon\,|0\rangle+\sin\epsilon\,|1\rangle)^{\otimes N}}{\sqrt{1+\cos^N\epsilon\sin(2\theta)}}, \tag{4.4}$$

with $0\leq\epsilon\leq\pi/2$ and $0\leq\theta\leq\pi/4$. The state $|\Xi(\theta,\epsilon)\rangle$ is just a product state when $\theta=0$ and becomes GHZ state if $\theta=\pi/4$ and $\epsilon=\pi/2$. The distance between two component states is given by the value of ϵ. The parametrization in ϵ for fixed $\theta=\pi/4$ was introduced in Ref. [33] and explored in Refs. [47, 66]. Since the state is permutation-symmetric, we can easily calculate quantum macroscopicity following the methods in Sec. 3.4.

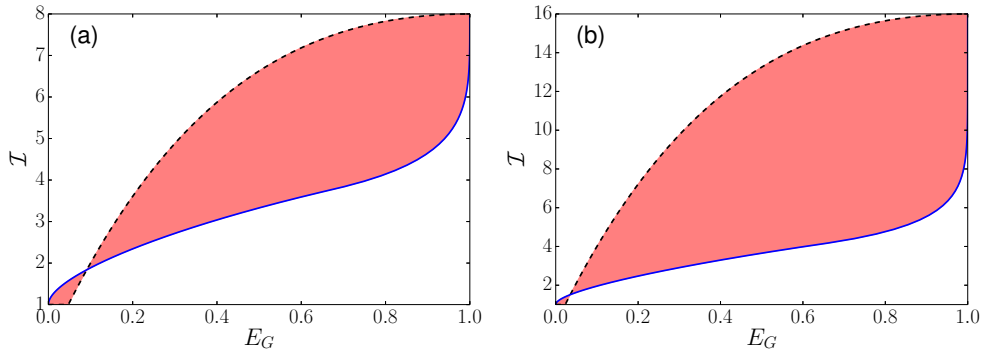

Figure 2: Normalized quantum macroscopicity as a function of geometric entanglement for the generalized GHZ states $|\Xi(\theta,\epsilon)\rangle$ for (a) $N = 8$ and (b) $N = 16$. The two extremal cases are given by $\epsilon = \pi/2$ (dashed) and $\theta = \pi/4$ (solid).

We note that for $\epsilon > \pi/2$, the destructive interference between the two amplitudes associated to the component $|0\rangle^{\otimes N}$ can lead to geometric entanglement larger than unity. For example, we obtain the W-state

$$|W\rangle_N = \frac{1}{\sqrt{N}}\left(|10\ldots0\rangle + |010\ldots0\rangle + \ldots|00\ldots01\rangle\right), \tag{4.5}$$

in the limit $\epsilon \to \pi, \theta \to \pi/4$, for odd N.

To calculate geometric entanglement of $|\Xi(\theta,\epsilon)\rangle$, we parametrize the closest separable state as

$$|\Phi_{\text{sep}}(\alpha)\rangle = \left(\cos\alpha\,|0\rangle + \sin\alpha\,|1\rangle\right)^{\otimes N}, \tag{4.6}$$

where the overlap with $|\Xi(\theta,\epsilon)\rangle$ is calculated as

$$|\,\langle\Phi_{\text{sep}}(\alpha)|\Xi(\theta,\epsilon)\rangle\,|^2 = \frac{(\cos\theta\cos^N\alpha + \sin\theta\cos^N(\epsilon-\alpha))^2}{1+\cos^N\epsilon\sin(2\theta)}. \tag{4.7}$$

We need to maximize with respect to α to obtain the value of geometric entanglement. For large N limit, the overlap is obviously maximized for $\alpha = 0$ (since $\theta \leq \pi/4$). For finite N, the maximum can conveniently be found numerically, since the overlap (4.7) does not oscillate fast as a function of α.

We show the behavior of geometric entanglement E_G and quantum macroscopicity $\mathcal{I}$ in Fig. 2, for two different numbers of qubits $N = 8$ and 16. Although quantum macroscopicity increases with geometric entanglement in general, the relationship is ambiguous. Especially for large numbers of qubits N, we can find a state which has the large value of geometric entanglement but small quantum macroscopicity. Our results from extensive numerical calculations show that the maximum macroscopicity for a given value of geometric entanglement is attained by the value obtained for $|\Xi(\theta = \pi/4, \epsilon)\rangle$ or $|\Xi(\theta, \epsilon = \pi/2)\rangle$, in the range $E_G \leq 1$.

When $\epsilon = \pi/2$, $0 \leq \theta \leq \pi/4$, geometric entanglement and quantum macroscopicity can be exactly calculated. Following Sec. 3.4, the VCM V is calculated as

$$V = \begin{pmatrix} 1 & 0 & 0 \\ 0 & 1 & 0 \\ 0 & 0 & N \sin^2 2\theta \end{pmatrix} \tag{4.8}$$

which yields the normalized macroscopicity $\mathcal{I} = \max(1, N \sin^2 2\theta)$. We also easily obtain the geometric entanglement which is given as $E_G = -\log_2(\cos^2 \theta)$. Therefore, we can see that for $0 < \theta \leq \arcsin \sqrt{1/N}/2$, the geometric entanglement give a finite value but normalized macroscopicity

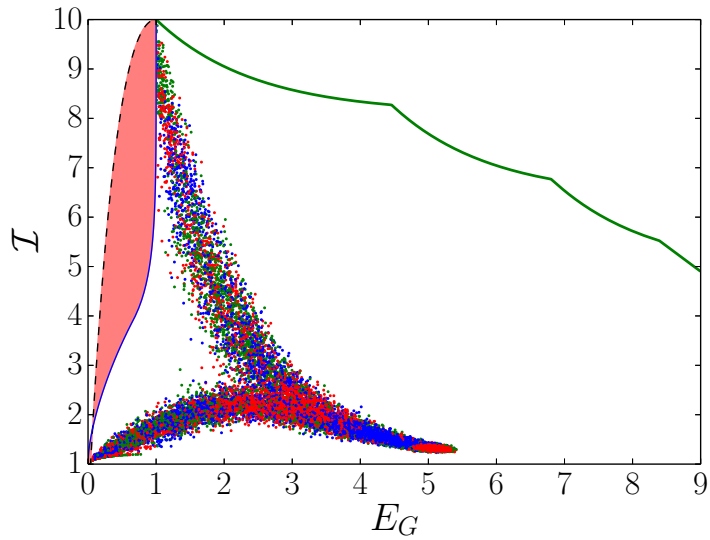

Figure 3: Geometric entanglement E_G versus normalized quantum macroscopicity $\mathcal{I}$ for a randomly generated entanglement states. For initial product state $|0\rangle^{\otimes N}$ and the GHZ state $|\mathrm{GHZ}\rangle_N$, we apply a random unitary gate $U \in \mathrm{SU}(4)$ to random two neighboring sites many times. The size of system $N = 10$ is used. Green curve indicates an upper bound of $\mathcal{I}$ for a given value of E_G obtained from the ansatz in Ref. [64].

is just 1 which is the same to the product states.

4.2.2 Far-from-separable states

Let us now move on strongly geometrically entangled states. We focus on a quantum state the maximal overlap with separable states η of which is smaller than $1/2$. It also implies that geometric entanglement $E_G = -\log_2 \eta$ has the value large than 1.

We first numerically investigate the relation between E_G and normalized quantum macroscopicity $\mathcal{I}$ using the set of randomly generated states. Starting from a product state $|0\rangle^{\otimes N}$ or the GHZ state $|\mathrm{GHZ}\rangle_N$, we apply a random

unitary gate $U \in \mathrm{U}(4)$ to i-th and $i+1$-th particles many times. The site i is also chosen randomly for each gate operation. The detailed generation scheme for these state can be found in Sec. 5.2.

Figure 3 displays E_G versus $\mathcal{I}$ for randomly generated states using this scheme. The size of system $N = 10$ is used. We see that geometric entanglement E_G generally increases as we apply random unitary gates regardless of the initial state we have chosen. However, the normalized quantum macroscopicity $\mathcal{I}$ shows the different behaviors depending on the initial states. When the initial state was $|0\rangle^{\otimes N}$, the values of $\mathcal{I}$ first slightly increases and it decreases next as we apply gate operations whereas the normalized macroscopicity continuously decreases when the initial state was $|\mathrm{GHZ}\rangle_N$.

From the result, we may expect that a quantum state cannot have the large values of both E_G and $\mathcal{I}$ (for example, $E_G > 6$ and $\mathcal{I} > 8$). Actually, this expectation holds generally. The large value of E_G means the large number of terms are required when expressed using any product basis. As the variance of a macroscopic observable has a large value when the outcome probabilities are concentrated only in several measurement outcomes where a distance between them is far, both quantity cannot be large at the same time. Precisely, if $E_G(|\psi\rangle) = -\log_2 \lambda$, the quantum state $|\psi\rangle$ is represented as

$$|\psi\rangle = \sum_{i=1}^{D} \sqrt{\lambda_i} e^{i\theta_i} |i\rangle_v \tag{4.9}$$

for $0 \leq \lambda_1 \leq \lambda_2 \leq \cdots \leq \lambda_D \leq \lambda$ and $\sum_i \lambda_i = 1$ where $D = 2^N$ is the dimension of the Hilbert space. In addition, $|i\rangle_v$ forms the basis of product

states

$$\left\{|i\rangle_v = |\phi_1^{(i)}\rangle \otimes |\phi_2^{(i)}\rangle \otimes \cdots \otimes |\phi_N^{(i)}\rangle : i \in [0, \cdots, D-1]\right\}. \tag{4.10}$$

The large value of E_G means the small value of λ which means λ_i are largely distributed among i. From this picture, an ansatz to obtain rough upper bound of $\mathcal{I}$ for given E_G is obtainable (details can be found in Ref. [64]). We display the bound obtained from the ansatz in Fig. 3.

Chapter 5

Quantum macroscopicity for random states[1]

In this chapter, we show that macroscopic quantum superpositions are rare in the Hilbert space of a many-particle system. Our results provide a kinematic picture why we cannot see macroscopic quantum superpositions in a macroscopic system.

5.1 Haar-random states

Before introducing Haar-random states, let us first consider random points in the unit sphere S^2. If we pick many points uniformly in the sphere following the probability density $(dS)/S$ where $dS = \sin\theta d\theta d\phi$ is the surface element, the resulting distribution will be invariant under any rotation of the unit sphere. Likewise, Haar-random states are the ensemble of pure quantum states that are uniformly (in the sense of the Haar-measure) distributed on the Hilbert space.

Haar-random states play special role in quantum information theory as they show the volume law of entanglement entropy and predict the properties of a thermal state. For example, Haar-random states of the Hilbert space spanned by the eigenstates in a energy shell of a given Hamiltonian provide a quantum picture corresponding to the microcanonical ensemble in statistical

[1]The contents of this chapter is largely based on the second part of Ref. [64]

mechanics [67, 68]. We here consider Haar-random states in the full Hilbert space of N spin-$1/2$ particles. This ensemble is invariant under the any unitary transformation in $\mathrm{U}(2^N)$. A quantum state in this ensemble can be seen as a pure thermal state of free particles or the infinite temperature.

5.1.1 State generation

Haar-random states in N particle spin-$1/2$ system can be constructed by randomly generating the real and imaginary parts of the coefficients $c_1, \cdots, c_{2^N}$ following a zero-mean unit-variance normal distribution in any fixed basis. The resulting unnormalized vector $\vec{c}$ is then normalized in a second step.

5.1.2 Macroscopicity is rare in Haar-random states

It is usual that a function for quantum states give almost the same values for random states. For a given Lipschitz-continuous function $f(|\Psi\rangle)$, the values of f remain close to the average value $\langle f \rangle$ for the vast majority of states. Formally, the probability for a deviation larger than ϵ is given as [69]

$$P[|f(|\psi\rangle) - \langle f \rangle| > \epsilon] \leq 4e^{-\frac{(n+1)\epsilon^2}{24\pi^2\eta^2}}, \tag{5.1}$$

where η is the Lipschitz constant. It is also known as Levy's lemma. As the expectation values of an observable as a function of quantum states is Lipschitz-continuous, the quantum macroscopicity defined in Eq. (3.1) is also Lipschitz-continuous while the geometric measure of entanglement inherits Lipschitz-continuity from the distance-like measure it is based on [70, 71, 72]. Hence,

most Haar-random states are very similar, both when characterized by their geometric entanglement and their quantum macroscopicity.

Random matrix theory [73] provides a method to predict various quantities for Haar-random states and have been used diverse contexts in physics [74, 75]. The typical magnitudes of the elements of the VCM (3.15) also can be calculated using random matrix theory [76]. In the limit $N \to \infty$, the VCM approaches the unit matrix [76] which means that the largest eigenvalues of V converge to unity. By the upper bound (3.17), the normalized quantum macroscopicity of a Haar-random state approaches to the minimum value 1.

In contrast, random states chosen according to the Haar measure possess large geometric entanglement [70, 71]: With probability greater than $1 - e^{-N^2}$, we have for $N \geq 11$ [70]

$$E_G(|\Psi_{\text{random}}\rangle) \geq N - 2\log_2 N - 3. \tag{5.2}$$

These results also certifies quantum macroscopicity and geometric entanglement are different kinds of quantumness. Geometric entanglement is a typical trait of quantum states whereas quantum macroscopicity is not.

5.1.3 Numerical results

We numerically reproduce the expected behavior of geometric entanglement E_G and normalized macroscopicity $\mathcal{I}$ as function of N in Fig. 4. In agreement with the previous argument, the geometric entanglement increases with the number of qubits N (a), while the normalized macroscopicity decays (b). We

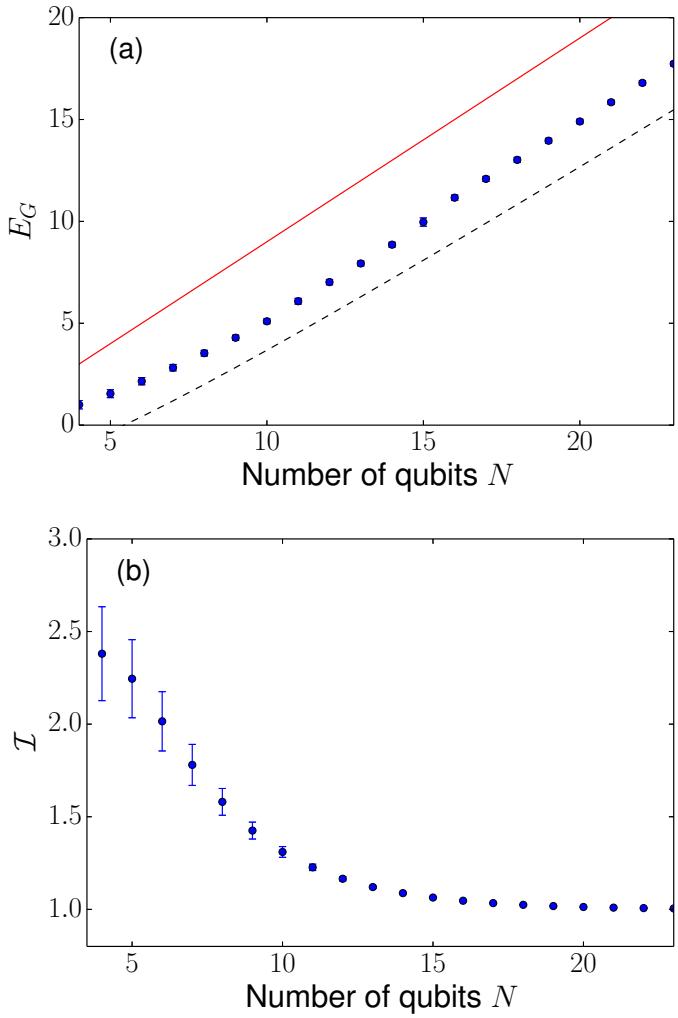

Figure 4: For Haar-random states in a N-particle spin-$1/2$ system, we calculate (a) averaged geometric entanglement and (b) averaged normalized quantum macroscopicity. In (a), solid line indicates an upper bound $E_G \leq N-1$ and dashed curve shows a lower bound Eq. (5.2). Error bars show the one standard deviation of the obtained numerical data. We can see that geometric entanglement continuously increases with the number of qubits whereas normalized macroscopicity decreases.

find that geometric entanglement E_G increases almost linearly in N whereas the decreasing behavior of $\mathcal{I}$ is rather complicated. In Ref. [64], it is shown that $(\mathcal{M} - N)/N(N-1)$ decrease exponentially in N. Therefore, the scaling behavior of the normalized quantum macroscopicity is given as $\mathcal{I} \sim (N-1)e^{-\gamma N} + 1$ for some decay constant γ. This is obviously $\mathcal{O}(1)$ which indicates the absence of macroscopic quantum superpositions.

We also plot E_G versus $\mathcal{I}$ for Haar-randomly generated states in Fig. 5. It directly shows that typical states in the Hilbert space of N spin-$1/2$ particles have a large geometric entanglement and small quantum macroscopicity.

5.2 Random physical states

In the above section, we have calculated two different quantumness (geometric entanglement E_G and normalized quantum macroscopicity $\mathcal{I}$) for Haar-random states. It also implies that a thermal pure state of a system of free particles may not a macroscopic superposition. However, there have been some arguments that Haar-random states are not physical even though the ensemble of Haar-random states well describes various properties of the thermal state. This is because exponentially many of N two-qubit gates are required to approach a random state in the Hilbert space from any product state [77]. To address this mismatch, the ensemble of random physical states have been suggested and investigated [78]. In this chapter, we numerically show that typically small value of $\mathcal{I}$ and large value of E_G can be obtainable in $\mathcal{O}(N^3)$ two qubit operations using the ensemble of random physical states.

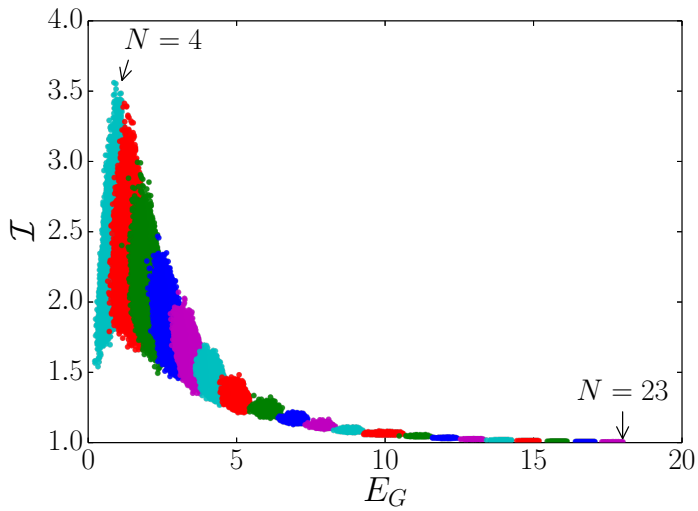

Figure 5: For numerically generated Haar-random states, we plot E_G versus $\mathcal{I}$ in a plane. As the system size N increases, geometric entanglement E_G increases whereas normalized quantum macroscopicity $\mathcal{I}$ decreases. Different colors are used to indicate different values of N.

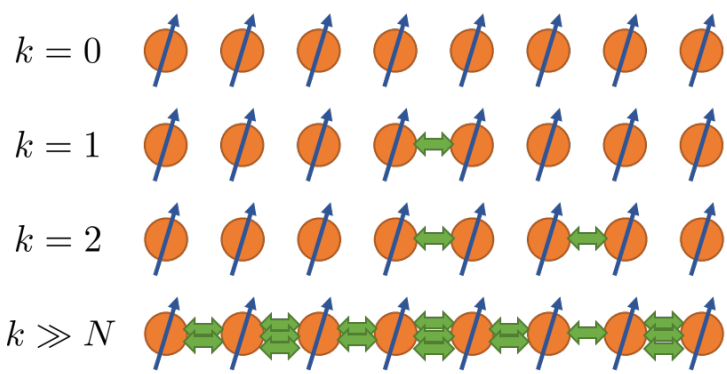

Figure 6: We apply k times a random unitary operation in $\mathrm{U}(4)$ between two randomly chosen adjacent sites (closed boundary conditions). For $k \gg N$, we have a fully connected system with high probability, i.e. the state is typically 0-separable, for $k \to \infty$, we reach the limit of Haar-uniform states.

5.2.1 State generation

Random physical state can be numerically obtained using the same method what we have seen in Sec. 4.2.2. Precisely, we first assume that the qubits are aligned in a one-dimensional spin-chain configuration. Random physical state $|\Psi_k\rangle$ is obtained after we apply k times a random two-qubit unitary gate onto a randomly chosen pair of two neighboring qubits. That is, for $k < N - 1$, the state remains at least 1-separable (the first qubit in the chain has never directly or indirectly interacted with the last one), while we obtain Haar-random states in the limit $k \gg N$, which we have discussed in the above Section 5.1. Figure 6 represents this scheme to generate random physical states.

5.2.2 Numerical results

Geometric entanglement and quantum macroscopicity for random physical states are shown in Fig. 7 as a function of the number of applied binary gates k. The results of four different values of $N = 4, 6, 13$ and 20 are displayed. Between $k \approx N$ and $k \approx N^2$, we observe a steep increase in the geometric entanglement of random physical states. It means that the state typically becomes fully inseparable for this range of numbers of binary interactions k. For $k \approx N^3$, we observe a saturation of both macroscopicity and geometric entanglement. While geometric entanglement increases monotonically with the number of applied gates, quantum macroscopicity develops a peaked structure. The maximum value of macroscopicity is reached for $N \leq k \leq N^2$. For this values of k, the states are probably not a separable state, nor they are highly complex (not exponentially many product states are required to express

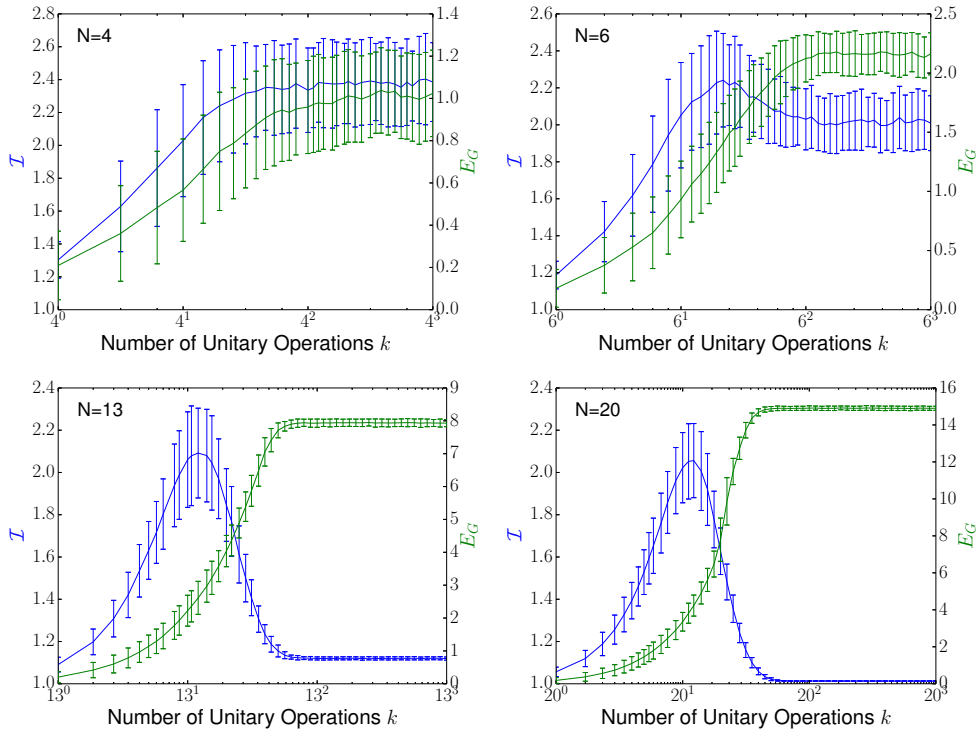

Figure 7: The averaged values of the geometric entanglement (green curves with error bars) and normalized quantum macrosocpicity (blue curves with error bars) for random physical states as a function of the number of applied two-qubit unitary gates k. Four different values of $N = 3, 6, 13$ and $N = 20$ are used. Standard deviations of the numerically obtained data are shown using the error bars. We can see that geometric entanglement generally increases with k for all N, but normalized quantum macroscopicity first increases but starts to decrease after some $N \leq k \leq N^2$ for $N \geq 6$.

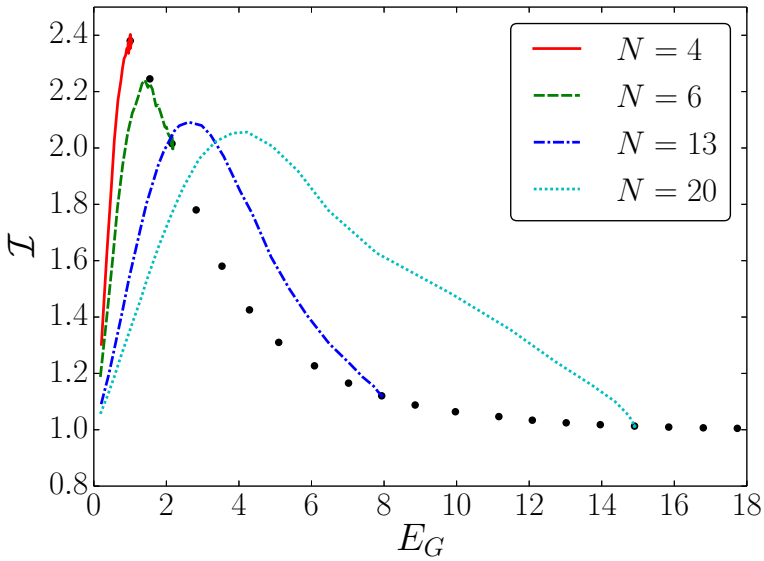

Figure 8: Average trajectories of random physical states $|\Psi_k\rangle$ in the $E_G - \mathcal{M}$-plane for $N = 4, 6, 13$,and 20. The curves start at $k = 1$ and proceed to $k = N^3$. Each point in a plane represents the averaged result for Haar-random states.

the states). These are the requirements for high macroscopicity.

We also display the trajectories of random physical states as a function of k in the $(\mathcal{M}, E_G)$-plane [Fig. 8] proceed from $k = 1$ to $k = N^3$ with the averaged values of Haar-random states. The averaged values for Haar-random states for $1 \leq N \leq 24$ are represented with points. It clearly shows that the values of the geometric entanglement E_G and normalized quantum macroscopicity $\mathcal{I}$ of Haar-random states are achievable within N^3 gate operations.

5.3 Remarks

In conclusion, we have shown that a random state in the Hilbert space of a N spin-$1/2$ particles typically has small quantum macroscopicity and large geo-

metric entanglement. Furthermore, the class of random states for the size of system N is not macroscopic superposition as $\mathcal{I} = O(1)$. We also have shown that the typical values of geometric entanglement and quantum macroscopicity are physically achievable using the ensemble of random physical states. Our result presents that macroscopic superpositions are very rare in the Hilbert space and cannot be easily obtainable from a product state using only neighboring interactions.

Chapter 6

Dynamics of entanglement and quantum macroscopicity in a closed many-body system

In the previous chapter, geometric entanglement and quantum macroscopicitiy are investigated for Haar-random states and random physical states. The results show that macroscopic superpositions are rare in the Hilbert space and the class of typical states for given system size N is not a macroscopic superposition. In this chapter, we investigate whether a similar result can be obtained from the unitary dynamics of a isolated system. A precise question which we will address in this chapter is that: Do initial macroscopic superpositions lose their size by unitary dynamics?

Of course, a quantum superposition in a closed system does not become a classical mixture as it does when environmental effects exist. However, it has been shown that expectation values of physical observables in isolated quantum systems tend to evolve into that of thermal ensemble, which is known as thermalization [79, 80, 81] (see Ref. [82] for a recent review).

We first show that if an N-particle system thermalizes, quantum macroscopicity $\mathcal{M}$ after thermalization is bounded by the order of N. This means that a system cannot be in a macroscopic quantum superposition after thermalization. We find that the suppression of the fluctuation of macroscopic observables

relative to the system size, which is due to thermalization, leads to this result. We also investigate the dynamics of quantum macroscopicity in many-body localized (MBL) systems which does not thermalize and have recently been experimentally realized [83, 84, 85]. We show that a macroscopic superposition can maintain the size of it after long time evolution.

Next, we numerically investigate a disordered XXZ chain which alters depending on the strength of the disordered magnetic filed [86] between the thermalization phase and the MBL phase that does not thermalize [87, 88, 89]. It consistently shows that a system cannot be in a macroscopic superposition in a long time scale if the system thermalizes while a localized system can.

6.1 Thermalization of a closed system and the size of the macroscopic superposition

When a system thermalizes, eigenstate thermalization hypothesis (ETH) can be employed to obtain the expectation value of an operator after thermalization. In this section, we calculate the long time averaged value of $\mathcal{V}_A(|\psi(t)\rangle)$ using the ETH for a macroscopic observable $A = \sum O_i \in S$ where we define $O_i = \vec{\alpha}_i \cdot \boldsymbol{\sigma}^{(i)}$ for the convenience and S is the set of macroscopic observables defined in Eq. (3.3). The basics of equilibration and thermalization of a closed system are summarized in Appendix B. As in the Appendix, we define the time averaged value of an observable as $\overline{O} = \int_0^\infty O(t)dt$ where $O(t) = \langle\psi|e^{iHt}Oe^{-iHt}|\psi\rangle$ is an expectation value of O at time t. We first assume that all local spin operators $\sigma_a^{(i)}$ and two body observables $\sigma_a^{(i)}\sigma_b^{(j)}$ for

$i, j \in \{1, \cdots, N\}$ and $a, b \in \{x, y, z\}$ satisfy the ETH. Under these assumptions, we obtain the time averaged values of A and A^2 as (see Appendix B for details)

$$\begin{aligned}
\overline{A} = \overline{\langle\psi(t)|A|\psi(t)\rangle} &= \sum_i \overline{O_i} = \sum_i \left[\langle O_i\rangle_{\mathrm{mc}} + \mathcal{O}(D^{-1/2})\right] \\
&= \sum_i \left[\langle O_i\rangle_T + \mathcal{O}(1/N)\right] \\
&= \sum_i \langle O_i\rangle_T + \mathcal{O}(1) \\
&= \langle A\rangle_T + \mathcal{O}(1) \qquad (6.1)
\end{aligned}$$

and

$$\begin{aligned}
\overline{A^2} = \overline{\langle\psi(t)|A^2|\psi(t)\rangle} &= \sum_{i,j} \overline{O_i O_j} \\
&= \sum_{i,j} \left[\langle O_i O_j\rangle_{\mathrm{mc}} + \mathcal{O}(D^{-1/2})\right] \\
&= \sum_{i,j} \left[\langle O_i O_j\rangle_T + \mathcal{O}(1/N)\right] \\
&= \langle A^2\rangle_T + \mathcal{O}(N) \qquad (6.2)
\end{aligned}$$

where D is the dimension of the Hilbert space, $\langle\cdot\rangle_{\mathrm{mc}}$ and $\langle\cdot\rangle_T$ are the micro-canonical ensemble and canonical ensemble averaged value of an observable, respectively.

The difference between $\overline{\langle\psi(t)|A|\psi(t)\rangle^2}$ and $\overline{A}^2$ is also needed to calculate the time averaged quantum fluctuation $\overline{\mathcal{V}_A}(|\psi(t)\rangle)$. We notice that this value is

small because

$$\overline{\langle\psi(t)|A|\psi(t)\rangle^2} - \overline{A}^2 = \lim_{\tau\to\infty}\frac{1}{\tau}\int_0^\tau \left(\langle A(t)\rangle - \overline{A}\right)^2$$
$$= \sum_{\alpha\neq\beta} |C_\alpha|^2|C_\beta|^2|\,\langle\alpha|A|\beta\rangle\,|^2$$

where the last expression is the averaged time fluctuation which is small when the equilibration occurs [90, 91, 92, 93]. Finally, we obtain the following relation between the quantum and the thermal fluctuations as

$$\overline{\mathcal{V}_A}(|\psi(t)\rangle) = \overline{\langle\psi(t)|A^2|\psi(t)\rangle} - \overline{\langle\psi(t)|A|\psi(t)\rangle^2} \tag{6.3}$$
$$= \langle A^2\rangle_T - \langle A\rangle_T^2 + \mathcal{O}(N). \tag{6.4}$$

When a system is in the thermal equilibrium, the fluctuation should be suppressed over the size of the system, i.e., $(\langle A^2\rangle_T - \langle A\rangle_T^2)/N^2 \to 0$ as N increases. In fact, for a typical non-critical system, $\langle A^2\rangle_T - \langle A\rangle_T^2$ behaves extensively so that it is $\mathcal{O}(N)$ [94]. For instance, a one-dimensional non-critical short-range interacting system has a finite thermal correlation length ξ, and the order of the correlation function is $\langle O_iO_j\rangle_T - \langle O_i\rangle_T\langle O_j\rangle_T \sim \mathcal{O}(e^{-|i-j|/\xi})$. The extensive behavior also can be regarded as a result of central limit theorem that works for this kind of system. Equation (6.4) then becomes $\overline{\mathcal{V}_A}(|\psi(t)\rangle) = \mathcal{O}(N)$ noting that $\langle A^2\rangle_T - \langle A\rangle_T^2 = \sum_{i,j}[\langle O_iO_j\rangle_T - \langle O_i\rangle_T\langle O_j\rangle_T]$. It immediately implies that $\mathcal{M}(|\psi(t)\rangle) = \mathcal{O}(N)$ and equivalently $\mathcal{I} = O(1)$ after thermalization. In other words, relaxed states after thermalization are no longer macroscopic superpositions even though initial states were macroscopic su-

perpositions. The Hamiltonian of such a system generally does not produce a macroscopic superposition and can be regarded as a classical process [51].

6.2 Dynamics of quantum macroscopicity in localized systems

When a system is fully localized, many local integrals of motion arise and they characterize the whole system. There are many different ways to choose the integrals of motions and their representations [95, 96]. We here follow "l-bits" representation in Ref. [96] as it is convenient to investigate the dynamical properties of the system (see e.g. Refs. [97, 98, 99]). In this representation, independent local integrals of motion are described using pseudospin operators that are connected to Pauli operators in physical basis with a quasi-local unitary transform. It means there are operators $\{\tau_z^i\}$ which commute with each others ($[\tau_z^i, \tau_z^j] = 0$ if $i \neq j$) and with the Hamiltonian ($[\tau_z^i, H] = 0$ for all i). In addition, there is a quasi-local unitary transform U such that $\tau_z^i = U\sigma_z^{(i)}U^\dagger$. Using this U, we also can define τ_x^i and τ_y^i. After constructing local integrals of motion, the Hamiltonian of many-body localized (MBL) systems can be written using these operators as

$$H = \sum_i \mathcal{E}_i \tau_z^i + \sum_{i,j} V_{i,j}\tau_z^i\tau_z^j + \sum_{i,j,k} V_{i,j,k}\tau_z^i\tau_z^j\tau_z^k + \cdots . \tag{6.5}$$

The interaction terms between τ_z^i which is absent in single particle localization (Anderson localization) makes distinguishing properties of a MBL system. They underlie many interesting dynamics of MBL systems such as logarithmic

increasing of bipartite entanglement [97], dephasing effects in local density operators and power-law decay of temporal fluctuations of local spins [98]. In contrast, single particle localized systems show freezing of bipartite entanglement and continuously fluctuating local spin expectation values.

Then let us calculate a lower bound of $\mathcal{M}(|\psi(t)\rangle)$ for $t \gg 1$ when a system is many-body localized. From the completeness of $\{\tau_a^i\}$, a local operator $O_i = \vec{\alpha}_i \cdot \boldsymbol{\sigma}^{(i)}$ can be expanded as

$$\begin{aligned} O_i &= \sum_{\{k,a\}} \gamma^i_{\{k,a\}} \tau^{k_1}_{a_1} \tau^{k_2}_{a_2} \cdots \tau^{k_n}_{a_n} \\ &= \sum_{k_1,a_1} \gamma^i_{k_1,a_1} \tau^{k_1}_{a_1} + \sum_{k_1,k_2,a_1,a_2} \gamma^i_{k_1,k_2,a_1,a_2} \tau^{k_1}_{a_1} \tau^{k_2}_{a_2} + \cdots \end{aligned} \tag{6.6}$$

where k, a runs over all subsets of $k \subset \{1, 2, \cdots, N\}$, $a = (a_1, a_2, \cdots, a_n)$ and $a_i \in \{x, y, z\}$ where $|k| = n$ (see e.g. Ref. [98, 99] which used the same expansion). Here, we can use the orthogonality of $\{\tau_a^i\}$ to obtain the coefficients $\gamma^i_{\{k,a\}}$. For example, the coefficient for τ_z^i is given as $\gamma^i_{i,z} = \mathrm{Tr}[O_i \tau_z^i]/2$. From the quasi-locality of U, the coefficients $\gamma^i_{\{k,a\}}$ decays as

$$\gamma^i_{\{k,a\}} \propto \exp[-\max(|k_\alpha - k_\beta|, |i - k_\alpha|)/\xi_2] \tag{6.7}$$

where maximum is taken over for all $\alpha, \beta \in \{1 \cdots N\}$ and ξ_2 is a characteristic length scale. To simplify notation, we now change into Heisenberg picture and omit ψ in the bra-ket as $\langle O(t)\rangle = \langle\psi(t)|O|\psi(t)\rangle$. In addition, we would define $T_a^k = \tau^{k_1}_{a_1} \tau^{k_2}_{a_2} \cdots \tau^{k_n}_{a_n}$. Then we can calculate the expectation value of $\langle A(t)\rangle$

when $A = \sum_i O_i$ as

$$\langle A(t)\rangle = \sum_{i=1}^{N} \langle O_i(t)\rangle = \sum_{i=1}^{N} \sum_{\{k,a\}} \gamma^i_{\{k,a\}} \langle T^k_a(t)\rangle \,. \tag{6.8}$$

Likewise, we also obtain

$$\begin{aligned}\langle A^2(t)\rangle &= \sum_{i,j=1}^{N} \langle O_i(t) O_j(t)\rangle \\ &= \sum_{i,j=1}^{N} \sum_{\{k,a\},\{l,b\}} \gamma^i_{\{k,a\}} \gamma^j_{\{l,b\}} \langle T^k_a(t) T^l_b(t)\rangle \,.\end{aligned} \tag{6.9}$$

Using these expressions, the variance of A is given by

$$\begin{aligned}&\mathcal{V}_A(|\psi(t)\rangle) = \langle A^2(t)\rangle - \langle A(t)\rangle^2 \\ &= \sum_{i,j=1}^{N} \sum_{\{k,a\},\{l,b\}} \gamma^i_{\{k,a\}} \gamma^j_{\{l,b\}} \left[\langle T^k_a(t) T^l_b(t)\rangle - \langle T^k_a(t)\rangle \langle T^{\{l\}}_{\{b\}}(t)\rangle\right] \\ &= \sum_{i,j=1}^{N} \sum_{a,b\in\{x,y,z\}} \gamma^i_{i,a} \gamma^j_{j,b} [\langle \tau^i_a(t) \tau^j_b(t)\rangle - \langle \tau^i_a(t)\rangle \langle \tau^j_b(t)\rangle] \\ &\quad + \sum_{i,j=1}^{N} \sum_{\substack{\{k,a\},\{l,b\} \\ k\neq\{i\}\vee l\neq\{j\}}} \gamma^i_{\{k,a\}} \gamma^j_{\{l,b\}} \left[\langle T^k_a(t) T^l_b(t)\rangle - \langle T^k_a(t)\rangle \langle T^l_b(t)\rangle\right].\end{aligned} \tag{6.10}$$

If a system is many-body localized, it is known that $\langle T^k_a(t)\rangle \propto 1/t^\kappa$ if $\exists a_i \in \{x, y\}$ where κ is a power law exponent [98]. Thus, only $a = z, b = z$ part contributes to the summation in the first term of Eq. (6.10) when $t \gg 1$. In addition, the second term of Eq. (6.10) consists of the operators more than

distance 1 from i and j. This term can be neglected when a system is deeply localized, $\xi_2 \ll 1$, as $\gamma^i_{\{k,a\}} \ll \gamma^i_{i,a}$ in this setting. To sum up, we obtain

$$\mathcal{V}_A(|\psi(t)\rangle) \approx \sum_{i,j=1}^{N} \gamma^i_{i,z}\gamma^j_{j,z}[\langle \tau^i_z \tau^j_z\rangle - \langle \tau^i_z\rangle \langle \tau^j_z\rangle] \tag{6.11}$$

in this limit. We dropped t from the right hand side as $\{\tau^i_z\}$ are constants of motion.

Then let us going back to the original Pauli operators basis. From the completeness of $\{\sigma^i_a\}$, we can write

$$\begin{aligned}\tau^i_z &= \sum_{\{k,a\}} \kappa^i_{\{k,a\}} \sigma^{k_1}_{a_1}\sigma^{k_1}_{a_1}\cdots\sigma^{k_1}_{a_1} \\ &= \vec{\beta}_i \cdot \boldsymbol{\sigma}^{(i)} + \sum_{\{k,a\},k\neq\{i\}} \kappa^i_{\{k,a\}} \sigma^{k_1}_{a_1}\sigma^{k_1}_{a_1}\cdots\sigma^{k_1}_{a_1}\end{aligned} \tag{6.12}$$

where we take out the $k = \{i\}$ term from the summation and

$$\vec{\beta}_i = \Big\{\mathrm{Tr}[\tau^i_z\sigma^{(i)}_x]/2, \mathrm{Tr}[\tau^i_z\sigma^{(i)}_y]/2, \mathrm{Tr}[\tau^i_z\sigma^{(i)}_z]/2\Big\}. \tag{6.13}$$

The norm of this vector is $|\vec{\beta}_i| \leq \mathrm{Tr}[(\tau^i_z)^2]/2 = 1$. In deep localized regime, we can neglect the second term in Eq. (6.12) and we obtain

$$\begin{aligned}&\sum_{i,j=1}^{N} \gamma^i_{i,z}\gamma^j_{j,z}[\langle \tau^i_z\tau^j_z\rangle - \langle \tau^i_z\rangle\langle \tau^j_z\rangle] \\ &\approx \sum_{i,j=1}^{N} \gamma^i_{i,z}\gamma^j_{j,z}|\vec{\beta}_i||\vec{\beta}_j|[\langle W_iW_j\rangle - \langle W_i\rangle\langle W_j\rangle]\end{aligned} \tag{6.14}$$

where $W_i = \hat{\beta}_i \cdot \boldsymbol{\sigma}^{(i)}$ and $\hat{\beta}_i = \vec{\beta}_i/|\vec{\beta}_i|$ is a unit vector of $\vec{\beta}_i$. In addition, from the expansion of Eq. (6.6) and the definition of O_i, we obtain $\gamma^i_{i,z} = \vec{\alpha}_i \cdot \vec{\beta}_i$. To obtain the simplified expression of Eq. (6.14), we consider the constant $c \geq 0$ which the set of equations

$$(\vec{\alpha}_i \cdot \vec{\beta}_i)|\vec{\beta}_i| = \pm c, |\vec{\alpha}_i| = 1 \text{ for all } i \in 1, 2, \cdots N \tag{6.15}$$

has the solution of $\{\vec{\alpha}_i\}$. For this solution, the right hand side of Eq. (6.14) is given as $c^2\mathcal{V}_B(|\psi(t=0)\rangle)$ where $B = \sum_i \text{sign}(\vec{\alpha}_i \cdot \vec{\beta}_i)W_i \in S$ is another macroscopic observable. As we want to give a lower bound of the right hand side, it is worth to consider the maximum possible value of c^2 over $\{\vec{\alpha}_i\}$. It is easy to show that the given set of equations does not have a solution if $c > \min_i |\vec{\beta}_i|^2$ as $|\vec{\alpha}_i \cdot \vec{\beta}_i| \leq |\vec{\beta}_i|$. In addition, $c = \min_i |\vec{\beta}_i|^2$ give a solution to Eq. (6.15) as $\vec{\alpha}_i = \pm(c/|\vec{\beta}_i|^2)\hat{\beta}_i + \vec{v}_i$ satisfy given set of equations for any $\vec{v}_i \perp \vec{\beta}_i$ which make $|\vec{\alpha}_i| = 1$. Therefore, for such solution of $\{\vec{\alpha}_i\}$, we obtain the following lower bound:

$$\mathcal{M}(|\psi(t)\rangle) \geq \mathcal{V}_A(|\psi(t)\rangle) \gtrsim c^2 \max_B \mathcal{V}_B(|\psi(t=0)\rangle) \tag{6.16}$$

where $A = \sum_i \vec{\alpha}_i \cdot \boldsymbol{\sigma}^{(i)}$, $c = \min_i |\vec{\beta}_i|^2 \leq 1$ and the maximum is taken over for all possible choices of sign for $B = \sum_i (\pm\hat{\beta}_i) \cdot \boldsymbol{\sigma}^{(i)}$. Here, the directions are given by $\vec{\beta}_i = \{\text{Tr}[\tau^i_z \sigma^{(i)}_x]/2, \text{Tr}[\tau^i_z \sigma^{(i)}_y]/2, \text{Tr}[\tau^i_z \sigma^{(i)}_z]/2\}$. We note that our lower bound depends on the value of $\mathcal{V}_B(|\psi(t=0)\rangle)$ therefore does not guarantee the large value of $\mathcal{M}(|\psi(t)\rangle)$ for $t \gg 1$ even when $\mathcal{M}(|\psi(t=0\rangle)$ is large if $\mathcal{V}_B(|\psi(t=0)\rangle)$ is small. In addition, note that we restricted our argument on

the deep localized regime. Our bound is sufficient in the context of this study but we expect that it may be possible to obtain more general lower bounds.

In contrast, let us consider a system which is just single particle localized so does not possess the interactions between pseudospins. In this case, correlation terms of Eq. (6.10) which contain τ_x^i or τ_y^i do not decay and oscillate permanently [98]. In other words, $a \neq z$ and $b \neq z$ terms in the first summation of Eq. (6.10) contribute to $\mathcal{V}_A(|\psi(t)\rangle)$ even when $t \gg 1$. Therefore, we expect that normalized quantum macroscopicity $\mathcal{I}(|\psi\rangle)$ preserves larger value than MBL case and continue to oscillate.

6.3 Numerical analysis using the disordered XXZ model

In the previous sections, we have investigated the expected values of normalized quantum macroscopicity $\mathcal{I}$ in thermalizing or MBL systems. In this section, we numerically verify those arguments. We consider the XXZ spin-1/2 chain model with a transverse field in the x direction and random fields along the z direction. The Hamiltonian of the system is given by

$$H = \sum_{i=1}^{N} \mathcal{J}_\perp (s_x^i s_x^{i+1} + s_y^i s_y^{i+1}) + \mathcal{J}_z s_z^i s_z^{i+1} + h_i s_z^i + \Gamma s_x^i \tag{6.17}$$

where $\mathcal{J}_\perp$ and $\mathcal{J}_z$ are the hopping and interaction strengths between two neighboring spins, respectively. A canonical spin-$1/2$ variable for the i-th spin is defined as $\boldsymbol{s}^i = \boldsymbol{\sigma}^{(i)}/2$ and $\{h_i\}$ and Γ describes disorder and transverse fields, respectively. We impose a periodic boundary condition $\boldsymbol{s}^{N+1} = \boldsymbol{s}^1$ and set

$\mathcal{J}_\perp = 1$ and $\hbar = 1$ throughout the chapter. Each h_i is an independent random variable picked up from a uniform distribution of $[-h, h]$ to describe the disorder field in the z direction, and the non-vanishing transverse field Γ in the x direction breaks the total symmetry of $J_z = \sum_i \sigma_i^z$.

When $\Gamma = 0$ and $\mathcal{J}_z = 0$, the Hamiltonian is directly mapped into non-interacting spinless fermions in a random potential $\sum_i c_{i+1}^\dagger c_i + h.c + h_i c_i^\dagger c_i$ using Wigner-Jordan transformation. This system is single particle localized for any non-vanishing h as it is the general property of non-interacting one-dimensional system with disorder [87].

In contrast, if $\mathcal{J}_z \neq 0$, the system is known to thermalize for small positive h and enters into the MBL phase when h increases. There have been many numerical studies in this model [86, 100, 101, 102]. These studies generally show that the value of h_c which yields MBL phase transition increases with $\mathcal{J}_z$. In addition, the transition point h_c have been numerically investigated for $\Gamma = 0$ and $\mathcal{J}_z = 1$, which is known as the disordered Heisenberg chain model. The results show that some eigenstates start to localize for $h \gtrsim 2.0$ and the whole eigenstates are localized for $h > h_c \approx 3.6$ in the sector of $J_z = 0$ for the finite N.

6.3.1 Initial random GHZ states in MBL systems

We first numerically calculate the behavior of the initial random GHZ states for the disordered Heisenberg model with small transverse field which can be obtained by setting $\mathcal{J} = \mathcal{J}_z = 1$ and $\Gamma = 0.1$ from Eq. (6.17). We intentionally added a small transverse field $\Gamma = 0.1\mathcal{J}$ as we want to break total J_z symmetry.

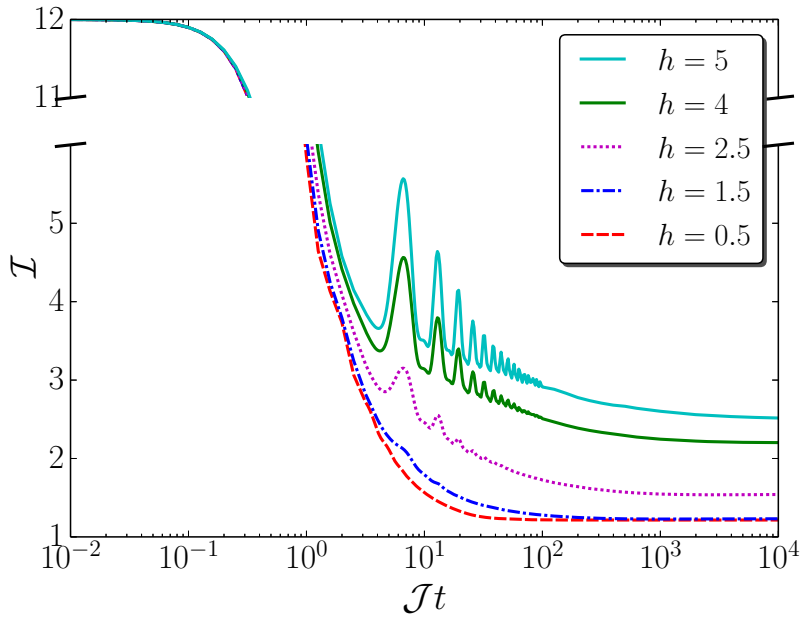

Figure 9: Time evolution of normalized quantum macroscopicity. For the disordered Heisenberg spin chain of size $N = 12$, we take average of $\mathcal{I}(|\psi(t)\rangle)$ over the disorder realizations and randomly chosen initial GHZ states. We then plot the results of the normalized quantum macroscopicity against time t. The dashed, dot-dashed, and dotted curves indicate the results for $h = 0.5$, $h = 1.5$, and $h = 2.5$, respectively, for which the eigenstates are fully delocalized ($h = 0.5$ and $h = 1.5$) or partially localized ($h = 2.5$). The results for $h = 4$ (lower) and $h = 5$ (upper) are indicated by the solid curves, which are the cases of the MBL phase. Obviously, $\mathcal{I}$ for the MBL cases converges to larger values than that for the thermalization cases does.

This small field does not make significant changes to the critical point of the MBL phase transition [103].

We fully diagonalize the Hamiltonian to characterize the time evolution of the system. We averaged over 10000 realizations of $\{h_i\}$ for $N = 6$, 1000 realizations for $N = 8$ and $N = 10$, and 200 realizations for $N = 12$ and $N = 14$. For each realization of $\{h_i\}$, we choose 100 random GHZ (Greenberger-Horne-Zeilinger) states for initial states and averaged all results. Each random GHZ

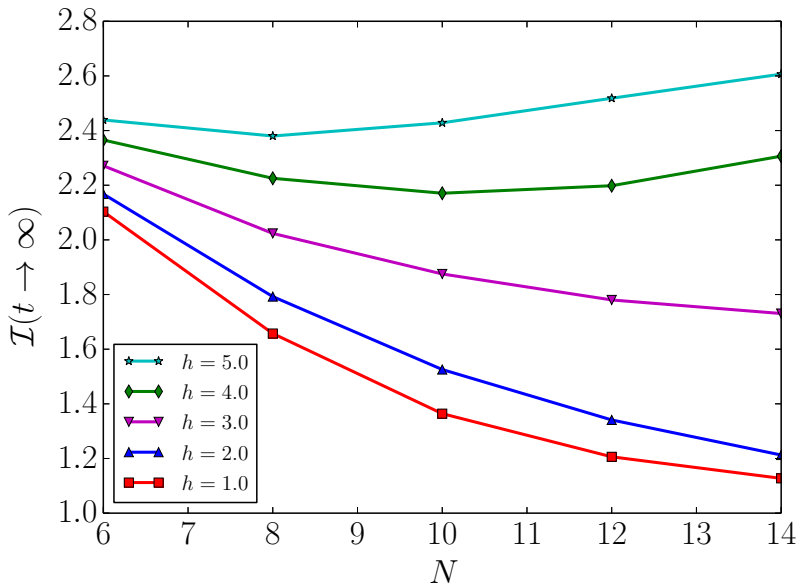

Figure 10: Saturated values of normalized quantum macroscopicity as a function of the system sizes. In thermal and intermediate region ($h < h_c \approx 3.6$), quantum macroscopicity of initial GHZ states is not preserved and $\mathcal{I}$ approaches 1 as N increases, which means $\mathcal{O}(N)$ behavior of $\mathcal{M}$. In contrast, we observe that $\mathcal{I}$ keeps increasing as N increases (i.e., $\mathcal{I} > \mathcal{O}(1)$) for the MBL phase ($h > h_c$).

state is constructed using $U_1 \bigotimes \cdots \bigotimes U_N \left|\mathrm{GHZ}\right\rangle_N$ where each U_i is a random unitary transform (in terms of Haar measure) in $\mathrm{SU}(2)$.

We numerically obtained the average values of the normalized quantum macroscopicity $\mathcal{I}$ for all realizations against time t for the system size $N = 12$ and plotted in Fig. 9. The starting value of $\mathcal{I}$ in Fig. 9 is 12 because $\mathcal{I} = N$ for the GHZ state.

Figure 9 shows that the saturated values of $\mathcal{I}$ for $t \gg 1$ in the MBL phase ($h > h_c$) are larger than those in $h < h_c$. The oscillations of $\mathcal{I}$ shown for $h \gtrsim 2.0$ in a certain time range are due to the oscillations of the spin correlation functions when the eigenstates are localized [98]. The average saturated values

of $\mathcal{I}$ as a function of N are plotted in Fig. 10. The average values of $\mathcal{I}$ decrease as N increases for $h < h_c$. This means that $\mathcal{M}(|\psi(t \gg 1)\rangle) = \mathcal{O}(N)$ and thus the initial random GHZ states in the thermalization phases have lost their properties as macroscopic quantum superpositions for $t \gg 1$. On the other hands, $\mathcal{I}$ increases as N increases in the cases of $h = 4$ and $h = 5$. This means that initial GHZ states in the MBL phase remain macroscopic quantum superpositions for $t \gg 1$.

We note that the normalized macroscopicity $\mathcal{I}$ decreases over N in the thermalization phase whereas it is known that the entanglement of entropy of $N/2$ concatenating regions in this system is proportional to N (the volume law of entanglement entropy). This also support our argument in Chapter 4 that quantum macroscopicity $\mathcal{I}$ captures a different kind of quantumness that can be small even when quantum states are largely entangled.

6.3.2 Comparison between many-body localized and single particle localized systems

In Sec. 6.2, we have argued that quantum macroscopicity in a single particle localized system may oscillate permanently and conserve larger values than a MBL case. To verify this argument, we numerically compare the dynamics of quantum macroscopicity between a single particle localized system and a many-body localized system. From the Hamiltonian Eq. (6.17), the same parameters $\mathcal{J}_z = 1$ and $\Gamma = 0.1$ with the above section are used for a MBL case but $\mathcal{J}_z = 0$ and $\Gamma = 0$ are used for a single particle localized system.

Figure 11(a) shows the averaged values of $\mathcal{I}$ as a function of time t for

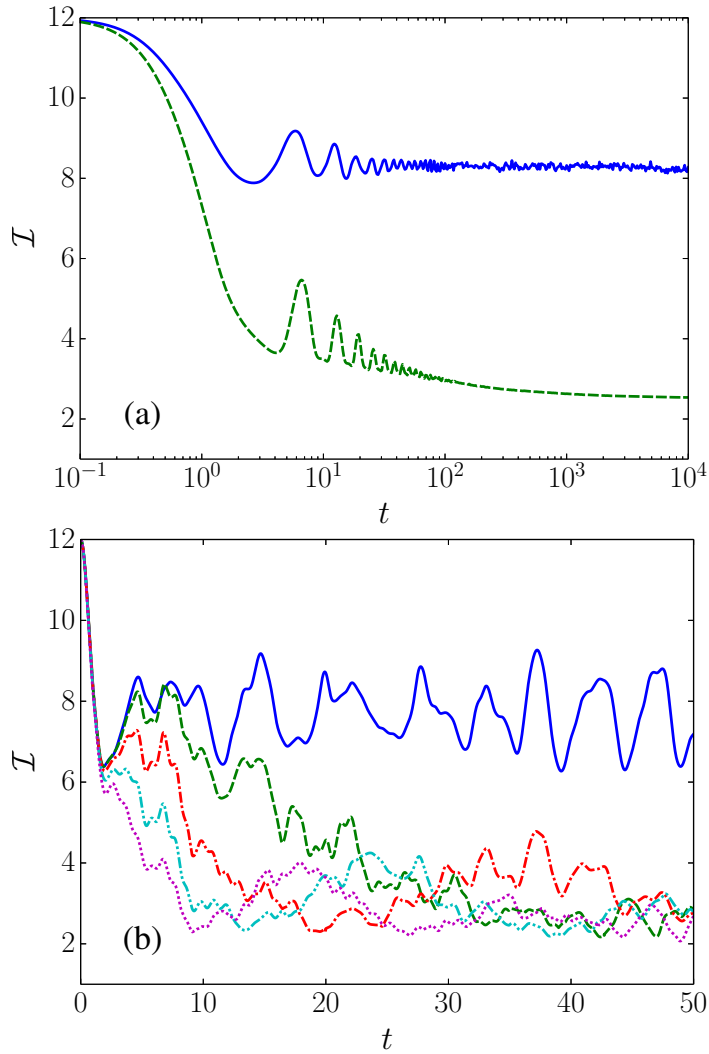

Figure 11: (a) Averaged value of normalized quantum macroscopicity $\mathcal{I}(|\psi(t)\rangle)$ over disorder realizations and initial states as a function of time. The solid curve shows the dynamics for a single particle localization system $\mathcal{J}_z = 0$ and $\Gamma = 0$ whereas the dashed curve corresponds to the dynamics for a MBL system, $\mathcal{J}_z = 1$ and $\Gamma = 0.1$ (see the Hamiltonian in Eq. (6.17)). Disorder strength $h = 5$ is used for the both cases. (b) Normalized quantum macroscopicity $\mathcal{I}(|\psi(t)\rangle)$ for a single random GHZ initial state against time t. Different values of interaction strength $\mathcal{J}_\perp = 0$, 0.1, 0.2, 0.3, 0.4 are indicated by solid, dashed, dot-dashed, dot-dot-dashed, and dotted curves, respectively. We set the disorder strength $h = 5$ and the vanishing transverse field $\Gamma = 0$. The dynamics of $\mathcal{I}$ for $\mathcal{J}_\perp = 0$ which corresponds to the single particle localization preserves the oscillation but it loses oscillating behavior for $\mathcal{J}_\perp > 0$.

these two different Hamiltonians for $N = 12$. We average over the 100 initial GHZ states in random local basis and 200 disorder realizations. In the single particle localization case (solid curve), we can see that the averaged value of $\mathcal{I}$ is preserved after initial oscillations whereas it decreases in the MBL case (dashed curve) even after the oscillations which is a signature of slow dephasing by interactions.

The loss of the oscillations in the single particle localized case is just an effect by on average over all realizations of disorders and initial states rather than true disappearance although that of the MBL case is due to a dephasing effect by the interactions that even can be seen for a single initial state. To explicitly support this argument, we display the normalized macroscopicity $\mathcal{I}$ for a single randomly generated initial GHZ state and a single disorder realization in Fig. 11(b) with different values of $\mathcal{J}_z$. The disorder strength $h = 5$ and the vanishing transverse field $\Gamma = 0$ are used. It directly shows that normalized quantum macroscopicity oscillates for a long time with a large amplitude and retains the larger value for $\mathcal{J}_z = 0$.

6.3.3 Initial rotated Néel GHZ states

We make deeper examinations of the dynamics and scaling behavior of $\mathcal{M}/N$ using a different set of initial states. We here consider rotated Néel GHZ states as initial states which are given by $|\psi(0)\rangle = U^{\otimes N} |\Psi_0\rangle$ where $U = e^{-I\sigma_y\theta/2}$ is a rotation about y axis with an angle θ and

$$|\Psi_0\rangle = (|\uparrow\downarrow\uparrow\downarrow\cdots\rangle + |\downarrow\uparrow\downarrow\uparrow\cdots\rangle)/\sqrt{2} \tag{6.18}$$

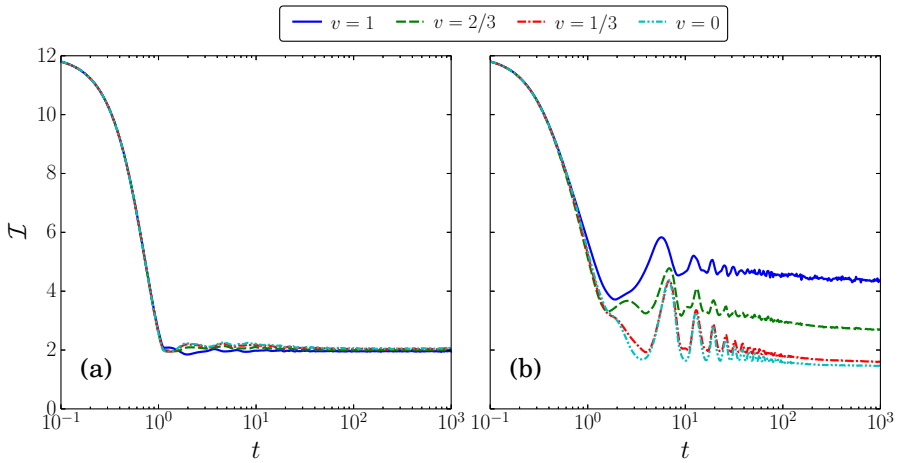

Figure 12: Averaged values of normalized quantum macorscopicity $\mathcal{I}(|\psi(t)\rangle)$ as time t for different values of $v = \cos\theta$ with the disorder strengths (a) $h = 1.0$ and (b) $h = 5.0$.

is a superposition between two different antiferromagnetic ordered Néel states. We let $\cos\theta = v$ which corresponds to z-coordinate of $U|\uparrow\rangle$ in the Bloch sphere. We use four different values of $v = 0$, $1/3$, $2/3$ and 1 to set the initial states. The value $v = 1$ means no rotation as $\theta = 0$, whereas $v = 0$ corresponds to the states which are aligned over x axis as $\theta = \pi/2$.

Using the Hamiltonian considered in Sec. 6.2, which is obtained from Eq. (6.17) by setting $\mathcal{J}_\perp = \mathcal{J}_z = 1$ and $\Gamma = 0.1$, we plot $\mathcal{I}$ as a function of time t in Fig. 12. The size of system $N = 12$ and four different values of v are used. The results show that $\mathcal{I}$ approach to the similar values as time evolves in the thermalization phase regardless of the value of v. In contrast, the converged values of $\mathcal{I}$ in the MBL phase increase with v.

We also plot the saturated values of $\mathcal{I}$ after equilibration as functions of N in Fig. 13. We find that $\mathcal{I}$ does not increase with N even for the MBL

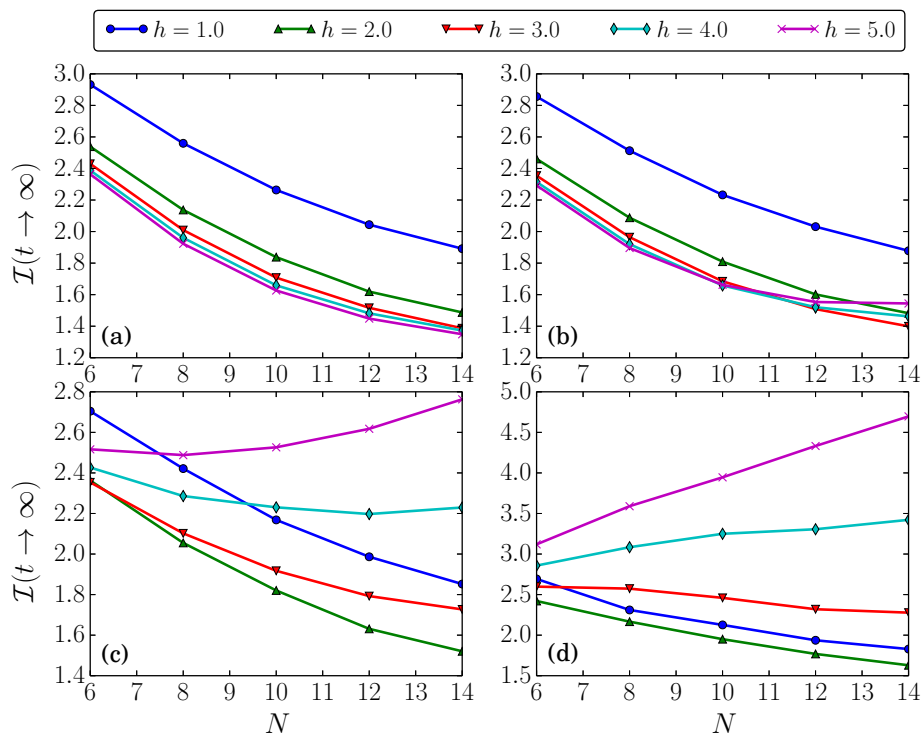

Figure 13: Averaged values of normalized quantum macorscopicity $\mathcal{I}(|\psi(t)\rangle)$ at time $t \gg 1$ as a function of the size of system N for (a) $v = 0$, (b) $v = 1/3$, (c) $v = 2/3$, and (d) $v = 1$. The results for different values of $h = 1.0$ to 5.0 are shown.

phase if the initial states are prepared with $v = 0$ [(a) case]. The lower bound Eq. (6.16) can give a hint to this behavior. In the case of vanishing transverse field, $\Gamma = 0$, conservation of the total spin-z operator $J_z = \sum_i \sigma_z^{(i)}$ makes $\hat{\beta}_i = \hat{z} = \{0, 0, 1\}$ [98]. Then for the combination of $B = \sum_i (\pm)\sigma_z^{(i)}$, we can simply calculate $\max_B \mathcal{V}_B(|\psi(t=0)\rangle) = N + (N^2 - N)\cos^2\theta$. As we expect that the small value of $\Gamma = 0.1$ does not make a significant difference, our lower bound indicates that the saturated values of $\mathcal{M}/N$ must increases as N increases for $v > 0$ but it can retain the small value for $v = 0$.

We next discuss a feasible experimental scheme to detect preservation of a macroscopic superposition in a MBL system. There have been several experimental realizations of MBL systems using optical lattices [83, 84] and trapped ion [85]. We here focus on a trapped-ion implementation [85] as trapped ions provide high controllability in preparation of initial states and measurement of various operators.

We first aware that the measurement of staggered magnetization in the rotated basis gives the maximum variance for rotated Néel GHZ states. Explicitly, the operator

$$S(\theta) = \sum_{i=1}^{N} (-1)^i \vec{\chi}_i \cdot \boldsymbol{\sigma}^{(i)} \tag{6.19}$$

where $\vec{\chi}_i = \{\sin\theta, 0, \cos\theta\}$ gives the maximum variance $\mathcal{V}_{S(\theta)}(U^{\otimes N}|\Psi_0\rangle) = N^2$. In addition, as $S(\theta)$ is a macroscopic observable, $\mathcal{M}(|\psi\rangle) \geq \mathcal{V}_{S(\theta)}(|\psi\rangle)$.

We calculated the saturated values of the variance of the operator $S(\theta)$ for the initial rotated Néel states as the size of the system N. The result is plotted

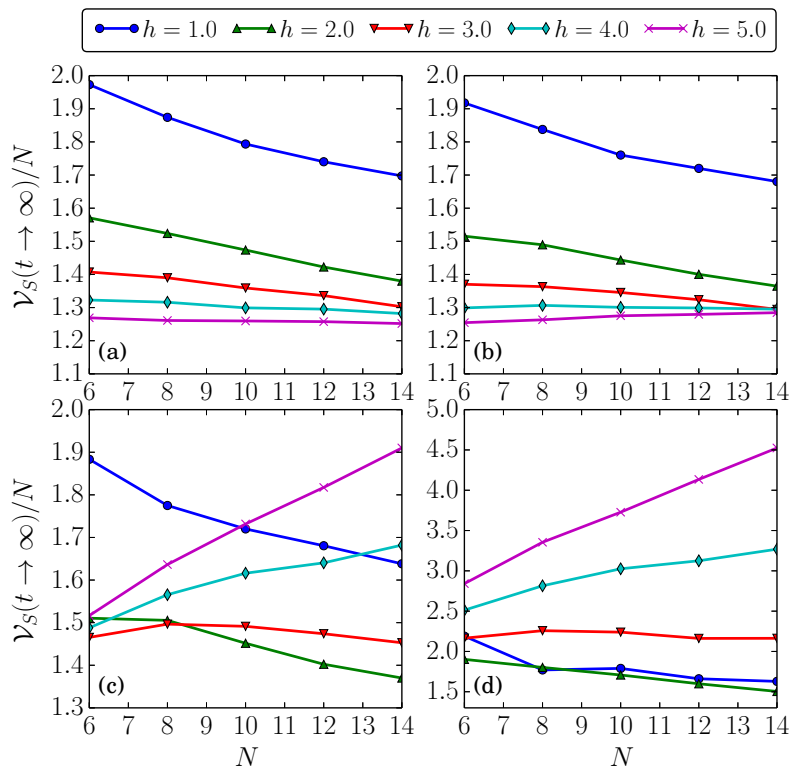

Figure 14: Averaged saturated values of the variance of staggered magnetization $S(\theta)$ in rotated basis versus the size of system N. Four different values of (a) $v = 0$, (b) $1/3$, (c) $2/3$, and (d) 1 are used. The staggered magnetisms in rotated basis $S(\theta)$ are sufficient to capture the behaviors of normalized quantum macroscopicity $\mathcal{I} = \max_A \mathcal{V}_A/N$ in MBL systems.

in Fig. 14. The results show the similar behavior with Fig. 13. Importantly, it shows the increasing behavior for $v = 1/3, 2/3, 1$ as N increases in the MBL phase. It means that we can see the preservation of quantum macroscopicity in the MBL phase only using the operator $S(\theta)$.

We finally comment that one can prepare an initial state $U^{\otimes N} |\Psi_0\rangle$ and measure $\mathcal{V}_{S(\theta)}$ in a trapped-ion system. First, the initial state of the form $U^{\otimes N} |\Psi_0\rangle$ can be prepared using trapped ions as GHZ states up to $N = 14$ can be arranged [104] and single qubit rotations with extreme high fidelity ($\approx 99.9999\%$) [105] can be applied consecutively. Subsequently, we evolute the system using the disordered Ising Hamiltonian with long-range interactions [85] for sufficient time $t \gg 1$. After that, we rotate all qubits into the original z basis and measure the staggered magnetization in z basis as in [85]. After repeating many measurements, the variance $\mathcal{V}_{S(\theta)}$ can be calculated.

Nevertheless, we here note that it is not simple to answer whether macroscopic superpositions would disappear in a trapped-ion quantum simulator as long-range interactions are present in this system. It requires a more detailed study to show that how long-range interactions affect the behavior of $\mathcal{V}_{S(\theta)}$.

6.4 Remarks

It is well known that a macroscopic superposition disappears in a short time due to decoherence caused by interactions with environments, while it is often believed that a macroscopic superposition would continue to survive as far as it is ideally isolated from its environment.

In this Chapter, we have investigated macroscopic superpositions in a

closed system under thermalization using the measure of quantum macroscopicity introduced in Chapter 3. Using the ETH, we have shown that the value of normalized quantum macroscopicity is the order of 1 for general non-critical short-range interacting spin systems. This means that the state after thermalization is not a macroscopic superposition any longer. In contrast, local integrals of motion arise in a MBL system may preserve the size of a macroscopic superposition.

We have also performed numerical analyses with the disordered XXZ spin chain varied by the strength of the disorder between the thermalization phase and the MBL phase without thermalization. Our numerical results confirm that macroscopic superpositions disappear when a closed system thermalizes, while they may be preserved in the case of MBL phase in which the system does not thermalize.

Our study reveals an important role of the suppression of quantum fluctuation in the thermalization process and explains why a macroscopic quantum superposition is hardly observed in a real world even without the assumption of openness of quantum systems.

Chapter 7

Conclusion

Even today, enormous resources are being invested to devise a bigger size of macroscopic quantum superposition in many laboratories over the world. Why they are so hard to be seen? Decoherence theory provides an answer to this question based on the assumption that our system of interest is interacting with a big incoherent bath. The interaction between systems diminishes the coherence in a superposition and this is usually believed the reason why we cannot see them. However, we can make an another question: Is it possible the bath is in a superposition of two macroscopically distinct states? Under the open system based picture, we should think a bath of this bath to answer the question. The questions continue until we consider the whole universe. To do not fall in this weird recursion of the questions, we have to consider an isolated system.

In this thesis, we have considered an isolated many-particle spin system to give some evidences that macroscopic superpositions are hardly seen even without the assumption of the openness of the system. We have used a measure to quantify the size of macroscopic superpositions, which is also known as "quantum macroscopicity" or "macroscopic quantumness." Starting from the definition of the measure, we reviewed the properties and possible operational meanings of it. The well-constructed measure is further used to investigate Haar-random states in the many-particle Hilbert space. The result shows that

macroscopic superpositions are very rare even for pure quantum states.

We also have investigated the dynamics of the measure in a closed system. Using the eigenstate thermalization hypothesis, we first show that the states after thermalization are not macroscopic superstitions. Many-body localized systems which do not thermalize are also analyzed to show that these systems can preserve quantum macroscopicity of an initial state. Extensive numerical results are also provided to show that initial macroscopic superpositions lose their size as time evolves in thermalizing systems whereas the size of superpositions is preserved in many-body localized systems.

In conclusion, using the well-established measure with various analytic and numerical techniques, we have shown that macroscopic superpositions are hard to be seen even in a closed many-body quantum system. There are some possible further works. For example, extending our results to other systems such as many-particle bosonic or fermionic systems, a single mode bosonic cavity, and large spin-S systems are good candidates. Moreover, experimental tests of the arguments presented in the thesis are also demanding. We expect such following works would deepen our understanding of macroscopic superpositions.

Appendix A

Big-O and big-Θ notations

Throughout the thesis, we have used big-O and big-Θ notations. We here define these notations. Formally, we say $f(n) \in \mathcal{O}(g(n))$ if and only if

$$\exists k > 0 \, \exists n_0 \text{ such that } |f(n)| \leq k|g(n)| \text{ for all } n > n_0. \tag{A.1}$$

Intuitively, it means $f(n)$ is below or the same order to $g(n)$. The overused notation $f(n) = \mathcal{O}(g(n))$ is also commonly used. Here, equal sign '=' does not present the real equality. For example, $x = \mathcal{O}(x^2)$ is true but $x^2 = \mathcal{O}(x)$ is false. We also have used $f(n) > \mathcal{O}(g(n))$ which means $f(n) \notin \mathcal{O}(f(n))$. It does not necessarily mean that $f(n)$ is bigger than $g(n)$ for most of n as $f(n)$ can be oscillating function. However, when we are only dealing with monotonically increasing $f(n)$ and $g(n)$, it means that $f(n)$ increases faster than $g(n)$. For example, $N^{1+\epsilon} > \mathcal{O}(N)$ for all $\epsilon > 0$.

Similarly, we say $f(n) \in \Theta(g(n))$ or equivalently, $f(n) = \Theta(g(n))$ if and only if

$$\exists k_1 > 0 \, \exists k_2 > 0 \exists n_0 \text{ such that } k_1 g(n) \leq f(n) \leq k_2 g(n) \text{ for all } n > n_0 \tag{A.2}$$

which means $f(n)$ and $g(n)$ are the same order.

Appendix B

Equilibration and thermalization

We briefly summarize equilibration and thermalization of a closed system (for a comprehensive review, see Ref. [82] and references therein. See also Ref. [106] for a short review). Let $|\alpha\rangle$ denote an eigenstate of Hamiltonian $\hat{H}$ with eigenvalue E_α. We consider α as an integer index and we assume that the eigenstates $|\alpha\rangle$ are sorted in ascending order by the value of energy E_α. For an initial state $|\psi(0)\rangle = \sum_\alpha C_\alpha |\alpha\rangle$, the state at time t is given by

$$|\psi(t)\rangle = \sum_\alpha C_\alpha e^{-iE_\alpha t} |\alpha\rangle ,$$

and the time-dependent expectation value of a local operator O is

$$\begin{aligned} \langle O(t)\rangle &= \langle\psi(t)|O|\psi(t)\rangle \\ &= \sum_\alpha |C_\alpha|^2 \langle\alpha|O|\alpha\rangle + \sum_{\alpha\neq\beta} C_\alpha^* C_\beta e^{i(E_\alpha - E_\beta)t} \langle\alpha|O|\beta\rangle . \end{aligned} \tag{B.1}$$

We first assume non-degenerate energies and energy gaps, and the time averaged value of $\langle O(t)\rangle$ is expressed as

$$\overline{O} = \lim_{\tau\to\infty} \frac{1}{\tau} \int_0^\tau dt \, \langle O(t)\rangle = \sum_\alpha |C_\alpha|^2 \langle\alpha|O|\alpha\rangle \tag{B.2}$$

using Eq. (B.1). This value is the same to $\mathrm{Tr}[\rho_D O]$ where $\rho_D = \sum_\alpha |C_\alpha|^2 |\alpha\rangle \langle\alpha|$ is a diagonal ensemble. The equilibration requires $\langle O(t)\rangle$ would be the same to the $\overline{O}$ for most of time t, and this means that the second term of Eq. (B.1) is small for general $t > 0$. There are two different arguments leading to this result. The first argument is based on the typicality, which shows that the second term is very small for typical initial states [91, 90, 92]. This argument is based on the distribution of coefficients $\{C_\alpha\}$ for typical states.

The eigenstate thermalization hypothesis (ETH) [79, 80] provides another argument for the equilibration. It states that $\langle\alpha|O|\beta\rangle$ is exponentially small in the system size when $\alpha \neq \beta$ and this leads to the smallness of the second term. This is one of the basic assumptions of ETH [93] and tested numerically in Refs. [81, 107, 108, 109]. In any cases, we can see the equilibration generally occurs. However, there is still a problem of equilibration time. The time required to equilibrate obtained from the above arguments is very large compared to that observed in numerical simulations and experiments. This is an interesting open question.

In addition to the equilibration, thermalization requires the expectation values of an observable to the same with the thermal ensemble averaged values. General mechanism of thermalization is still been investigating. However, we know that the ETH can be used to predict the physical quantities when a closed quantum system thermalizes. Many studies on various many-body systems have shown that the ETH is satisfied for local operators or two-point correlation functions [81, 107, 110, 108, 111, 112, 113, 114, 115, 116, 117, 109, 118].

The ETH assumes that the diagonal elements in energy basis $\langle\alpha|O|\alpha\rangle$ vary slowly as a function of E_α where the difference between neighboring diagonal components $\langle\alpha+1|O|\alpha+1\rangle - \langle\alpha|O|\alpha\rangle$ is exponentially small in the size of the system. We then define the total energy $\bar{E} = \sum_\alpha |C_\alpha|^2 E_\alpha$. The microcanonical ensemble average can be expressed as

$$\langle O\rangle_{\rm mc} = \frac{1}{\mathcal{N}_{\bar{E},\Delta E}} \sum_{|E_\alpha - \bar{E}|\leq \Delta E} \langle\alpha|O|\alpha\rangle$$

where $\mathcal{N}_{\bar{E},\Delta E}$ is number of states in the energy window centered at $\bar{E}$ and width ΔE. The summation is applied only for the energy eigenstates in this window defined by $\bar{E}$ and ΔE. It is known that the diagonal ensemble Eq. (B.2) approaches the microcanonical ensemble average for $(\Delta E)^2|O''(E)/O(E)| \ll 1$ where $O(E)$ is the expectation value of observable $\langle\alpha|O|\alpha\rangle$ as the function of energy E_α. Note that $O(E)$ is a smooth function in the thermodynamic limit from the ETH.

Actual numerical tests on diagonal ensembles and microcanonical ensembles for local operators and few-body operators show that they differ only in the order of $D^{-1/2}$ where D is the dimension of the full Hilbert space [107, 108, 114, 115, 116]. Therefore we can say $\overline{O} = \langle O\rangle_{\rm mc} + \mathcal{O}(D^{-1/2})$.

The diagonal ensemble and the canonical ensemble averaged values of theses observables are also compared. Under the ETH assumption, the difference between two ensembles for observables which do not depend on the size of the system (intensive observables) is given by $\mathcal{O}(1/N)$ where N is the size of the system [119]. More direct comparison between two ensembles using

numerical calculations for Bose-Hubbard model can be found in Ref. [116].

Bibliography

[1] A. Einstein, B. Podolsky, and N. Rosen, "Can quantum-mechanical description of physical reality be considered complete?," *Physical review*, vol. 47, no. 10, p. 777, 1935.

[2] E. Schrödinger, "Die gegenwärtige situation in der quantenmechanik," *Naturwissenschaften*, vol. 23, no. 48, pp. 807–812, 1935.

[3] J. S. Bell, "On the Einstein Podolsky Rosen paradox," *Physics*, vol. 1, no. 3, pp. 195–200, 1964.

[4] A. J. Leggett and A. Garg, "Quantum mechanics versus macroscopic realism: Is the flux there when nobody looks?," *Physical Review Letters*, vol. 54, no. 9, p. 857, 1985.

[5] C. Emary, N. Lambert, and F. Nori, "Leggett–garg inequalities," *Reports on Progress in Physics*, vol. 77, no. 1, p. 016001, 2013.

[6] M. Arndt and K. Hornberger, "Testing the limits of quantum mechanical superpositions," *Nature Physics*, vol. 10, no. 4, pp. 271–277, 2014.

[7] F. Fröwis, N. Sangouard, and N. Gisin, "Linking measures for macroscopic quantum states via photon–spin mapping," *Optics Communications*, vol. 337, pp. 2–11, 2015.

[8] W. H. Zurek, "Decoherence, einselection, and the quantum origins of the classical," *Reviews of modern physics*, vol. 75, no. 3, p. 715, 2003.

[9] M. B. Plenio and S. Virmani, "An introduction to entanglement measures," *Quantum Information & Computation*, vol. 7, p. 1, 2007.

[10] L. Amico, R. Fazio, A. Osterloh, and V. Vedral, "Entanglement in many-body systems," *Reviews of Modern Physics*, vol. 80, no. 2, p. 517, 2008.

[11] R. Horodecki, P. Horodecki, M. Horodecki, and K. Horodecki, "Quantum entanglement," *Reviews of modern physics*, vol. 81, no. 2, p. 865, 2009.

[12] E. Schrödinger, "Discussion of probability relations between separated systems," in *Mathematical Proceedings of the Cambridge Philosophical Society*, vol. 31, pp. 555–563, Cambridge Univ Press, 1935.

[13] R. F. Werner, "Quantum states with einstein-podolsky-rosen correlations admitting a hidden-variable model," *Physical Review A*, vol. 40, no. 8, p. 4277, 1989.

[14] S. Popescu, "Bell's inequalities and density matrices: revealing "hidden" nonlocality," *Physical Review Letters*, vol. 74, no. 14, p. 2619, 1995.

[15] A. Peres, "Collective tests for quantum nonlocality," *Physical Review A*, vol. 54, no. 4, p. 2685, 1996.

[16] A. K. Ekert, "Quantum cryptography based on bell's theorem," *Physical review letters*, vol. 67, no. 6, p. 661, 1991.

[17] C. H. Bennett and S. J. Wiesner, "Communication via one-and two-particle operators on einstein-podolsky-rosen states," *Physical review letters*, vol. 69, no. 20, p. 2881, 1992.

[18] C. H. Bennett, G. Brassard, C. Crépeau, R. Jozsa, A. Peres, and W. K. Wootters, "Teleporting an unknown quantum state via dual classical and einstein-podolsky-rosen channels," *Physical review letters*, vol. 70, no. 13, p. 1895, 1993.

[19] C. H. Bennett, G. Brassard, S. Popescu, B. Schumacher, J. A. Smolin, and W. K. Wootters, "Purification of noisy entanglement and faithful teleportation via noisy channels," *Physical review letters*, vol. 76, no. 5, p. 722, 1996.

[20] C. H. Bennett, D. P. DiVincenzo, J. A. Smolin, and W. K. Wootters, "Mixed-state entanglement and quantum error correction," *Physical Review A*, vol. 54, no. 5, p. 3824, 1996.

[21] V. Vedral, M. B. Plenio, M. A. Rippin, and P. L. Knight, "Quantifying entanglement," *Physical Review Letters*, vol. 78, no. 12, p. 2275, 1997.

[22] M. A. Nielsen, "Conditions for a class of entanglement transformations," *Physical Review Letters*, vol. 83, no. 2, p. 436, 1999.

[23] W. Dür, G. Vidal, and J. I. Cirac, "Three qubits can be entangled in two inequivalent ways," *Physical Review A*, vol. 62, no. 6, p. 062314, 2000.

[24] M. J. Donald, M. Horodecki, and O. Rudolph, "The uniqueness theorem for entanglement measures," *Journal of Mathematical Physics*, vol. 43, no. 9, pp. 4252–4272, 2002.

[25] J. Eisert, M. Cramer, and M. B. Plenio, "Colloquium: Area laws for the entanglement entropy," *Reviews of Modern Physics*, vol. 82, no. 1, p. 277, 2010.

[26] J. Eisert and H. J. Briegel, "Schmidt measure as a tool for quantifying multiparticle entanglement," *Physical Review A*, vol. 64, no. 2, p. 022306, 2001.

[27] H. Barnum and N. Linden, "Monotones and invariants for multi-particle quantum states," *Journal of Physics A: Mathematical and General*, vol. 34, no. 35, p. 6787, 2001.

[28] T.-C. Wei and P. M. Goldbart, "Geometric measure of entanglement and applications to bipartite and multipartite quantum states," *Physical Review A*, vol. 68, no. 4, p. 042307, 2003.

[29] R. Hübener, M. Kleinmann, T.-C. Wei, C. González-Guillén, and O. Gühne, "Geometric measure of entanglement for symmetric states," *Physical Review A*, vol. 80, no. 3, p. 032324, 2009.

[30] A. Streltsov, H. Kampermann, and D. Bruß, "Simple algorithm for computing the geometric measure of entanglement," *Physical Review A*, vol. 84, no. 2, p. 022323, 2011.

[31] H. Jeong, M. Kang, and H. Kwon, "Characterizations and quantifications of macroscopic quantumness and its implementations using optical fields," *Optics Communications*, vol. 337, pp. 12–21, 2015.

[32] A. J. Leggett, "Macroscopic quantum systems and the quantum theory of measurement," *Progress of Theoretical Physics Supplement*, vol. 69, pp. 80–100, 1980.

[33] W. Dür, C. Simon, and J. I. Cirac, "Effective size of certain macroscopic quantum superpositions," *Physical review letters*, vol. 89, no. 21, p. 210402, 2002.

[34] J. R. Friedman, V. Patel, W. Chen, S. Tolpygo, and J. E. Lukens, "Quantum superposition of distinct macroscopic states," *nature*, vol. 406, no. 6791, pp. 43–46, 2000.

[35] C. H. Van der Wal, A. Ter Haar, F. Wilhelm, R. Schouten, C. Harmans, T. Orlando, S. Lloyd, and J. Mooij, "Quantum superposition of macroscopic persistent-current states," *Science*, vol. 290, no. 5492, pp. 773–777, 2000.

[36] A. Shimizu and T. Miyadera, "Stability of quantum states of finite macroscopic systems against classical noises, perturbations from environments, and local measurements," *Physical review letters*, vol. 89, no. 27, p. 270403, 2002.

[37] R. Haag, *Local quantum physics: Fields, particles, algebras*. Springer Science & Business Media, 2012.

[38] F. Strocchi, "Spontaneous symmetry breaking in quantum systems," *Scholarpedia*, vol. 7, no. 1, p. 11196, 2012.

[39] S. Yang and H. Jeong, "Relation between the greenberger-horne-zeilinger–entanglement cost of preparing a multipartite pure state and its quantum discord," *Physical Review A*, vol. 92, no. 2, p. 022322, 2015.

[40] S. Yang. (private communication).

[41] A. Shimizu and T. Morimae, "Detection of macroscopic entanglement by correlation of local observables," *Physical review letters*, vol. 95, no. 9, p. 090401, 2005.

[42] P. G. L. Mana *et al.*, "A size criterion for macroscopic superposition states," *Journal of Optics B: Quantum and Semiclassical Optics*, vol. 6, no. 11, p. 429, 2004.

[43] E. G. Cavalcanti and M. Reid, "Signatures for generalized macroscopic superpositions," *Physical review letters*, vol. 97, no. 17, p. 170405, 2006.

[44] J. I. Korsbakken, K. B. Whaley, J. Dubois, and J. I. Cirac, "Measurement-based measure of the size of macroscopic quantum superpositions," *Physical Review A*, vol. 75, no. 4, p. 042106, 2007.

[45] F. Marquardt, B. Abel, and J. von Delft, "Measuring the size of a quantum superposition of many-body states," *Physical Review A*, vol. 78, no. 1, p. 012109, 2008.

[46] C.-W. Lee and H. Jeong, "Quantification of macroscopic quantum superpositions within phase space," *Physical review letters*, vol. 106, no. 22, p. 220401, 2011.

[47] F. Fröwis and W. Dür, "Measures of macroscopicity for quantum spin systems," *New Journal of Physics*, vol. 14, no. 9, p. 093039, 2012.

[48] C.-Y. Park, M. Kang, C.-W. Lee, J. Bang, S.-W. Lee, and H. Jeong, "Quantum macroscopicity measure for arbitrary spin systems and its application to quantum phase transitions," *Physical Review A*, vol. 94, no. 5, p. 052105, 2016.

[49] J. Kofler and Č. Brukner, "Condition for macroscopic realism beyond the leggett-garg inequalities," *Physical Review A*, vol. 87, no. 5, p. 052115, 2013.

[50] J. Kofler and Č. Brukner, "Classical world arising out of quantum physics under the restriction of coarse-grained measurements," *Physical review letters*, vol. 99, no. 18, p. 180403, 2007.

[51] J. Kofler and Č. Brukner, "Conditions for quantum violation of macroscopic realism," *Physical review letters*, vol. 101, no. 9, p. 090403, 2008.

[52] F. Fröwis, P. Sekatski, and W. Dür, "Detecting large quantum fisher information with finite measurement precision," *Physical review letters*, vol. 116, no. 9, p. 090801, 2016.

[53] C.-Y. Park and H. Jeong, "Disappearance of macroscopic superpositions in perfectly isolated systems by thermalization processes," *arXiv preprint arXiv:1606.07213*, 2016.

[54] H. Kwon, C.-Y. Park, K. C. Tan, and H. Jeong, "Disturbance-based measure of macroscopic coherence," *arXiv preprint arXiv:1608.01122*, 2016.

[55] B. Yadin and V. Vedral, "General framework for quantum macroscopicity in terms of coherence," *Physical Review A*, vol. 93, no. 2, p. 022122, 2016.

[56] S. D. Bartlett, T. Rudolph, and R. W. Spekkens, "Reference frames, superselection rules, and quantum information," *Reviews of Modern Physics*, vol. 79, no. 2, p. 555, 2007.

[57] I. Marvian and R. W. Spekkens, "Extending noether's theorem by quantifying the asymmetry of quantum states," *Nature communications*, vol. 5, 2014.

[58] D. Poulin, "Macroscopic observables," *Physical Review A*, vol. 71, no. 2, p. 022102, 2005.

[59] T. Volkoff, "Nonclassical properties and quantum resources of hierarchical photonic superposition states," *Journal of Experimental and Theoretical Physics*, vol. 121, no. 5, pp. 770–784, 2015.

[60] A. Peres, *Quantum theory: concepts and methods*, vol. 57. Springer Science & Business Media, 2006.

[61] T. Morimae, A. Sugita, and A. Shimizu, "Macroscopic entanglement of many-magnon states," *Physical Review A*, vol. 71, no. 3, p. 032317, 2005.

[62] P. Hyllus, O. Gühne, and A. Smerzi, "Not all pure entangled states are useful for sub-shot-noise interferometry," *Physical Review A*, vol. 82, no. 1, p. 012337, 2010.

[63] R. Fletcher, *Practical methods of optimization*. John Wiley & Sons, 2013.

[64] M. C. Tichy, C.-Y. Park, M. Kang, H. Jeong, and K. Mølmer, "Macroscopic entanglement in many-particle quantum states," *Physical Review A*, vol. 93, no. 4, p. 042314, 2016.

[65] T. Morimae, "Superposition of macroscopically distinct states means large multipartite entanglement," *Physical Review A*, vol. 81, no. 1, p. 010101, 2010.

[66] T. Volkoff and K. Whaley, "Macroscopicity of quantum superpositions on a one-parameter unitary path in hilbert space," *Physical Review A*, vol. 90, no. 6, p. 062122, 2014.

[67] S. Popescu, A. J. Short, and A. Winter, "Entanglement and the foundations of statistical mechanics," *Nature Physics*, vol. 2, no. 11, pp. 754–758, 2006.

[68] P. Reimann, "Typicality for generalized microcanonical ensembles," *Physical review letters*, vol. 99, no. 16, p. 160404, 2007.

[69] M. Ledoux, *The concentration of measure phenomenon*. No. 89, American Mathematical Soc., 2005.

[70] D. Gross, S. T. Flammia, and J. Eisert, "Most quantum states are too entangled to be useful as computational resources," *Physical review letters*, vol. 102, no. 19, p. 190501, 2009.

[71] M. J. Bremner, C. Mora, and A. Winter, "Are random pure states useful for quantum computation?," *Physical review letters*, vol. 102, no. 19, p. 190502, 2009.

[72] M. Tiersch, *Benchmarks and statistics of entanglement dynamics*. PhD thesis, University of Freiburg, 2009.

[73] T. Tao, *Topics in random matrix theory*, vol. 132. American Mathematical Society Providence, RI, 2012.

[74] H. Weidenmüller and G. Mitchell, "Random matrices and chaos in nuclear physics: nuclear structure," *Reviews of Modern Physics*, vol. 81, no. 2, p. 539, 2009.

[75] F. Haake, *Quantum signatures of chaos*, vol. 54. Springer Science & Business Media, 2013.

[76] A. Sugita and A. Shimizu, "Correlations of observables in chaotic states of macroscopic quantum systems," *Journal of the Physical Society of Japan*, vol. 74, no. 7, pp. 1883–1886, 2005.

[77] D. Poulin, A. Qarry, R. Somma, and F. Verstraete, "Quantum simulation of time-dependent hamiltonians and the convenient illusion of hilbert space," *Physical review letters*, vol. 106, no. 17, p. 170501, 2011.

[78] A. Hamma, S. Santra, and P. Zanardi, "Quantum entanglement in random physical states," *Physical review letters*, vol. 109, no. 4, p. 040502, 2012.

[79] J. Deutsch, "Quantum statistical mechanics in a closed system," *Physical Review A*, vol. 43, no. 4, p. 2046, 1991.

[80] M. Srednicki, "Chaos and quantum thermalization," *Physical Review E*, vol. 50, no. 2, p. 888, 1994.

[81] M. Rigol, V. Dunjko, and M. Olshanii, "Thermalization and its mechanism for generic isolated quantum systems," *Nature*, vol. 452, no. 7189, pp. 854–858, 2008.

[82] C. Gogolin and J. Eisert, "Equilibration, thermalisation, and the emergence of statistical mechanics in closed quantum systems," *Reports on Progress in Physics*, vol. 79, no. 5, p. 056001, 2016.

[83] M. Schreiber, S. S. Hodgman, P. Bordia, H. P. Lüschen, M. H. Fischer, R. Vosk, E. Altman, U. Schneider, and I. Bloch, "Observation of many-body localization of interacting fermions in a quasirandom optical lattice," *Science*, vol. 349, no. 6250, pp. 842–845, 2015.

[84] J.-y. Choi, S. Hild, J. Zeiher, P. Schauß, A. Rubio-Abadal, T. Yefsah, V. Khemani, D. A. Huse, I. Bloch, and C. Gross, "Exploring the many-body localization transition in two dimensions," *Science*, vol. 352, no. 6293, pp. 1547–1552, 2016.

[85] J. Smith, A. Lee, P. Richerme, B. Neyenhuis, P. W. Hess, P. Hauke, M. Heyl, D. A. Huse, and C. Monroe, "Many-body localization in a quantum simulator with programmable random disorder," *Nature Physics*, vol. 12, 2016.

[86] A. Pal and D. A. Huse, "Many-body localization phase transition," *Physical review b*, vol. 82, no. 17, p. 174411, 2010.

[87] P. W. Anderson, "Absence of diffusion in certain random lattices," *Physical review*, vol. 109, no. 5, p. 1492, 1958.

[88] D. Basko, I. Aleiner, and B. Altshuler, "Metal–insulator transition in a weakly interacting many-electron system with localized single-particle states," *Annals of physics*, vol. 321, no. 5, pp. 1126–1205, 2006.

[89] R. Nandkishore and D. A. Huse, "Many body localization and thermalization in quantum statistical mechanics," *Annual Review of Condensed Matter Physics*, vol. 6, p. 15, 2015.

[90] N. Linden, S. Popescu, A. J. Short, and A. Winter, "Quantum mechanical evolution towards thermal equilibrium," *Physical Review E*, vol. 79, no. 6, p. 061103, 2009.

[91] P. Reimann, "Foundation of statistical mechanics under experimentally realistic conditions," *Physical review letters*, vol. 101, no. 19, p. 190403, 2008.

[92] A. J. Short, "Equilibration of quantum systems and subsystems," *New Journal of Physics*, vol. 13, no. 5, p. 053009, 2011.

[93] M. Srednicki, "Thermal fluctuations in quantized chaotic systems," *Journal of Physics A: Mathematical and General*, vol. 29, no. 4, p. L75, 1996.

[94] L. D. Landau and E. M. Lifshitz, *Statistical Physics, part 1*. Butterworth-Heinemann, 3 ed., 1980.

[95] M. Serbyn, Z. Papić, and D. A. Abanin, "Local conservation laws and the structure of the many-body localized states," *Physical review letters*, vol. 111, no. 12, p. 127201, 2013.

[96] D. A. Huse, R. Nandkishore, and V. Oganesyan, "Phenomenology of fully many-body-localized systems," *Physical Review B*, vol. 90, no. 17, p. 174202, 2014.

[97] A. Nanduri, H. Kim, and D. A. Huse, "Entanglement spreading in a many-body localized system," *Physical Review B*, vol. 90, no. 6, p. 064201, 2014.

[98] M. Serbyn, Z. Papić, and D. A. Abanin, "Quantum quenches in the many-body localized phase," *Physical Review B*, vol. 90, no. 17, p. 174302, 2014.

[99] A. Chandran, I. H. Kim, G. Vidal, and D. A. Abanin, "Constructing local integrals of motion in the many-body localized phase," *Physical Review B*, vol. 91, no. 8, p. 085425, 2015.

[100] D. J. Luitz, N. Laflorencie, and F. Alet, "Many-body localization edge in the random-field heisenberg chain," *Physical Review B*, vol. 91, no. 8, p. 081103, 2015.

[101] R. Vasseur, S. Parameswaran, and J. Moore, "Quantum revivals and many-body localization," *Physical Review B*, vol. 91, no. 14, p. 140202, 2015.

[102] M. Serbyn, Z. Papić, and D. A. Abanin, "Criterion for many-body localization-delocalization phase transition," *Physical Review X*, vol. 5, no. 4, p. 041047, 2015.

[103] Z.-C. Yang, C. Chamon, A. Hamma, and E. R. Mucciolo, "Two-component structure in the entanglement spectrum of highly excited states," *Physical review letters*, vol. 115, no. 26, p. 267206, 2015.

[104] T. Monz, P. Schindler, J. T. Barreiro, M. Chwalla, D. Nigg, W. A. Coish, M. Harlander, W. Hänsel, M. Hennrich, and R. Blatt, "14-qubit entanglement: Creation and coherence," *Physical Review Letters*, vol. 106, no. 13, p. 130506, 2011.

[105] T. Harty, D. Allcock, C. Ballance, L. Guidoni, H. Janacek, N. Linke, D. Stacey, and D. Lucas, "High-fidelity preparation, gates, memory, and readout of a trapped-ion quantum bit," *Physical review letters*, vol. 113, no. 22, p. 220501, 2014.

[106] J. Eisert, M. Friesdorf, and C. Gogolin, "Quantum many-body systems out of equilibrium," *Nature Physics*, vol. 11, no. 2, pp. 124–130, 2015.

[107] M. Rigol, "Quantum quenches and thermalization in one-dimensional fermionic systems," *Physical Review A*, vol. 80, no. 5, p. 053607, 2009.

[108] L. F. Santos and M. Rigol, "Localization and the effects of symmetries in the thermalization properties of one-dimensional quantum systems," *Physical Review E*, vol. 82, no. 3, p. 031130, 2010.

[109] W. Beugeling, R. Moessner, and M. Haque, "Off-diagonal matrix elements of local operators in many-body quantum systems," *Physical Review E*, vol. 91, no. 1, p. 012144, 2015.

[110] M. Rigol and L. F. Santos, "Quantum chaos and thermalization in gapped systems," *Physical Review A*, vol. 82, no. 1, p. 011604, 2010.

[111] T. N. Ikeda, Y. Watanabe, and M. Ueda, "Eigenstate randomization hypothesis: Why does the long-time average equal the microcanonical average?," *Physical Review E*, vol. 84, no. 2, p. 021130, 2011.

[112] R. Steinigeweg, J. Herbrych, and P. Prelovšek, "Eigenstate thermalization within isolated spin-chain systems," *Physical Review E*, vol. 87, no. 1, p. 012118, 2013.

[113] R. Steinigeweg, A. Khodja, H. Niemeyer, C. Gogolin, and J. Gemmer, "Pushing the limits of the eigenstate thermalization hypothesis towards mesoscopic quantum systems," *Physical review letters*, vol. 112, no. 13, p. 130403, 2014.

[114] T. N. Ikeda, Y. Watanabe, and M. Ueda, "Finite-size scaling analysis of the eigenstate thermalization hypothesis in a one-dimensional interacting bose gas," *Physical Review E*, vol. 87, no. 1, p. 012125, 2013.

[115] W. Beugeling, R. Moessner, and M. Haque, "Finite-size scaling of eigenstate thermalization," *Physical Review E*, vol. 89, no. 4, p. 042112, 2014.

[116] S. Sorg, L. Vidmar, L. Pollet, and F. Heidrich-Meisner, "Relaxation and thermalization in the one-dimensional bose-hubbard model: A case study for the interaction quantum quench from the atomic limit," *Physical Review A*, vol. 90, no. 3, p. 033606, 2014.

[117] H. Kim, T. N. Ikeda, and D. A. Huse, "Testing whether all eigenstates obey the eigenstate thermalization hypothesis," *Physical Review E*, vol. 90, no. 5, p. 052105, 2014.

[118] T. N. Ikeda and M. Ueda, "How accurately can the microcanonical ensemble describe small isolated quantum systems?," *Physical Review E*, vol. 92, no. 2, p. 020102, 2015.

[119] M. Srednicki, "The approach to thermal equilibrium in quantized chaotic systems," *Journal of Physics A: Mathematical and General*, vol. 32, no. 7, p. 1163, 1999.

국문초록

슈뢰딩거의 유명한 고양이 역설에서 볼 수 있듯, 거시적으로 다른 두 물체 간의 중첩은 양자역학에서 금지되지는 않지만 실제 일상생활에서는 보이지 않는다. 결 흘림 이론은 이 모순을 설명하는 가장 잘 알려진 주장이다. 이 이론은 우리가 보는 계와 환경 또는 저장체라고 불리는 다른 커다란 계 사이의 상호작용을 기초로 한다. 이러한 열린계를 기초로 하는 논거는 보통의 계에 대해서는 충분하지만, 환경이 이미 결 흘려진 열평형 상태에 있다고 가정하기 때문에 개념적으로 불완전하다.

본 논문에서는 계의 열림 가정 없이, 왜 거시중첩을 보기 힘든지에 대해서 탐구한다. 우리는 많은 입자계의 정역학과 동역학에 기초한 두 가지 다른 관점을 제시한다. 스핀-1/2인 많은 입자계의 순수한 양자 상태에 대하여 제한해 논의를 간단하게 한다. 처음으로, 우리는 해당 계에 대한 양자 거시성에 대한 척도를 도입하고 이를 기하학적 얽힘의 척도와 비교한다. 다음으로는 무작위 행렬에 대한 해석적인 관측과 대규모의 수치계산을 통해 많은입자 힐베르트 공간의 임의의 양자 상태는 전형적으로 적은 거시양자성만을 가짐을 보인다. 해당 결과는 우리가 왜 거시계에서 슈뢰딩거 고양이를 보지 못하느냐의 질문에 대한 정역학적인 답변을 준다.

비슷한 결과는 계의 동역학을 통해서도 얻을 수 있다. 먼저 닫힌계의 열평화에 대한 개념을 도입하고 고유상태 열화 가설을 이용하여 열평화화 이후의 양자상태는 작은 거시양자성만을 가짐을 보인다. 또한 열평화하거나 다체 국소화되는 무질서한 XXZ 모형에 대한 대규모 수치계산을 수행한다. 해당 계산결과는 열평화하는 계에서는 긴 시간이 흐른 뒤의 양자 상태는 일

반적으로 거시양자중첩이 아니라고 일관성 있게 나타내고, 열평형이 되지 않는 다체 국소화계 에서는 초기 상태의 양자중첩의 크기가 보존됨을 보인다.

주요어 : 거시양자중첩, 거시 양자 결맞음, 양자 상태의 전형성, 열평형화, 다체 국소화
학번 : 2010-23146